



Depositional Setting and Structural Evolution of the Archean Perseverance Volcanogenic Massive Sulfide Deposit, Matagami Mining District, Quebec, Canada

Samuel Pierre,^{1,†} Michel Jébrak,¹ Stéphane Faure,² and Gilles Roy³

¹ *Université du Québec à Montréal, Département des Sciences de la Terre et de l'Atmosphère, CP 8888, suc. Centre Ville, Montréal, Québec H3C 3P8, Canada*

² *CONSOREM Consortium de Recherche en Exploration Minérale, Université du Québec à Montréal, Montréal, Québec H3C 3P8, Canada*

³ *Glencore Canada Corporation, 8801 route Transcanadienne, Saint-Laurent, Québec H4S 1Z6, Canada*

Abstract

The Perseverance volcanogenic massive sulfide deposit (5.1 Mt at @ 15.8% Zn, 1.24% Cu, 29.4 g/t Ag, 0.4 g/t Au), Matagami district, Abitibi greenstone belt, consists of four pipelike orebodies discordant to local bedding in a shallow-dipping portion of the South Flank volcanic succession. Most of the ore is hosted by rhyolitic lavas of the Watson unit (2725.9 ± 0.8 Ma) and is overlain by a thinly laminated tuffaceous unit known as the Key Tuffite, as well as by rhyodacitic lavas of the Dumagami unit (2725.4 ± 0.7 Ma).

The presence of sulfide zones predominantly hosted in the footwall rhyolite, relicts of Key Tuffite within the ore, and intricate sulfide replacement of the laminated tuff are all features consistent with the formation of most of the deposit via seafloor replacement. The permeability of steep synvolcanic structures likely controlled the migration of metal-bearing fluids and simultaneously allowed the downward infiltration of seawater, causing mixing, cooling, and sulfide deposition in the seafloor environment. Stratigraphic relationships suggest that massive sulfide formation was active at Perseverance while tuffaceous sedimentation was ongoing on the seafloor. Progressive growth of the massive sulfides along subvertical structures was accompanied by the development of pipelike sericite-chlorite (± talc) alteration halos. Both the hanging wall and the footwall units are characterized by significant MgO mass gains, K₂O-Na₂O mass losses, and high alteration index values (e.g., chlorite-carbonate-pyrite index, alteration index). However, these geochemical changes are less intense and widespread in the hanging wall than in the footwall. The record of a decreasing alteration above the orebodies was likely caused by the emplacement of the rhyodacite while massive sulfide deposition and hydrothermal activity were still ongoing.

Primary relationships between mineralization and the host lithofacies were overprinted by intense deformation during the main event of compression induced by regional north-south shortening. Deformation is controlled by contrasting rheologies within the sulfide assemblage and between the orebodies and their host rocks. Structural modifications include the transposition of sulfide ores subparallel to the main foliation, the formation of piercement veins at the interface with the host rocks, and the generation of a series of secondary textures within the orebodies, including a vertical mineralogical banding. The distribution of Cu in the deposit is interpreted to be affected by the mechanical remobilization of chalcopyrite during deformation, whereas the zonation of Zn is likely primary. Hydrothermal alteration halos adjacent to the orebodies have accommodated significant strain, as indicated by the presence of tight folds in the Key Tuffite unit and a marked schistosity. Strain localization in the vicinity of the deposit highlights the relative ductility of the ore assemblage with respect to the host volcanic succession and resulted in a spatial association between hydrothermal alteration and deformation, despite the lack of a genetic relationship.

Introduction

Volcanogenic massive sulfide (VMS) deposits of the Matagami district (Quebec, Canada) are often quoted as a classic example of exhalative-style mineralization in a seafloor setting (Lavallière et al., 1994; Ioannou and Spooner, 2007; Ross et al., 2014). The exhalative model is mainly based on the close spatial relationship existing between VMS deposits and a thinly laminated tuffaceous marker known as the Key Tuffite, and on the interpretation that this unit is dominantly exhalative in origin (Davidson 1977; Liaghat and MacLean 1982). More recently, Genna et al. (2014) showed that the unit corresponds to a homogeneous calc-alkaline andesitic tuff progressively deposited in the water column, rather than an exhalite. Volcanogenic massive sulfide deposits located in the most fertile part of the district (i.e., South Flank area) are generally noted for their weak deformation and for the preservation of

their original characteristics (Lavallière et al., 1994; Ioannou and Spooner, 2007). In contrast to this interpretation, Roberts (1975) pointed out the structural complexity of the volcanic succession in proximity to the largest deposit of the district (i.e., Matagami Lake). Reconstructing the depositional environment of these deposits and identifying their degree of deformation during subsequent tectonic processes are critical for future exploration in the district, where limited outcrop exposures complicate the comprehension of the volcanic architecture.

The Perseverance deposit was discovered in 2001 and production occurred between 2008 and 2013 with premining resources of 5.1 million metric tons (Mt) at 15.8% Zn, 1.24% Cu, 29.4 g/t Ag, and 0.4 g/t Au (Arnold, 2006). The deposit is located in the western part of the South Flank area and consists of four pipelike massive sulfide bodies discordant to local bedding in a low-dipping portion of the volcanic succession. This setting is atypical for the district, where the

[†] Corresponding author: e-mail, spierre@mines.edu

deposits are either mound shaped in a moderately dipping succession or tabular shaped in a steeply dipping succession. It constitutes an excellent opportunity to characterize the relationships between mineralization and the host lithofacies as well as the structural modifications related to postdepositional deformation. The present paper reports on a detailed study constraining the stratigraphic and structural setting of the Perseverance deposit, describes the nature of hydrothermal alteration using mass-balance calculations, and emphasizes the physical behavior of the sulfide assemblage during deformation. A reconstruction of the successive stages in the evolution of the deposit is proposed.

Regional Geologic Setting

The Matagami mining district (Fig. 1) is located ~200 km to the northeast of Rouyn-Noranda within the northernmost volcanic succession of the Archean Abitibi greenstone belt. A total of 49.6 Mt of ore was produced in the district from 1963 to 2014, including 4.6 Mt Zn and 0.44 Mt Cu (G. Roy, pers. commun., 2014), making it the second most important Archean Zn district in Abitibi after Timmins (Hannington et al., 1999). Twenty VMS deposits ranging in size from ~0.1 to >25 Mt (i.e., Mattagami Lake) have been discovered in the district, of which 13 have been put into production

(Mercier-Langevin et al., 2014). The deposits are typically Zn rich, averaging ~9 wt % Zn, and contain as much as 18.7 wt % Zn (i.e., Isle-Dieu). Numerous studies have contributed to the geologic understanding of the district, with regional descriptions by Sharpe (1968), Beaudry and Gaucher (1986), Piché et al. (1993) and Pilote et al. (2011).

Volcanogenic massive sulfide deposits are hosted in a bimodal volcanic sequence consisting of a lower, dominantly felsic volcanic assemblage, the Watson Lake Group and overlain by a dominantly mafic volcanic assemblage, the Wabasse Group. The Watson Lake Group comprises (1) a lower poorly exposed, >500-m-thick, Fe-rich tholeiitic dacite (Liaghat and MacLean, 1992; Piché et al., 1993), and (2) an upper, >1,500-m-thick, massive tholeiitic rhyolite (Watson rhyolite), dated at 2725.9 ± 0.8 Ma (Ross et al., 2014). Both units display evidence of submarine volcanic emplacement, with hyaloclastites, autobreccias, and lobes (Beaudry and Gaucher, 1986; Arnold, 2006; Debreil, 2014).

A thinly laminated tuffaceous interval referred to as the Key Tuffite marks the transition to the Wabasse Group and can be traced across the entire district with a thickness ranging between several centimeters and 10 m (Liaghat and MacLean, 1992). Previously interpreted to be largely exhalative in composition, the Key Tuffite is now considered to

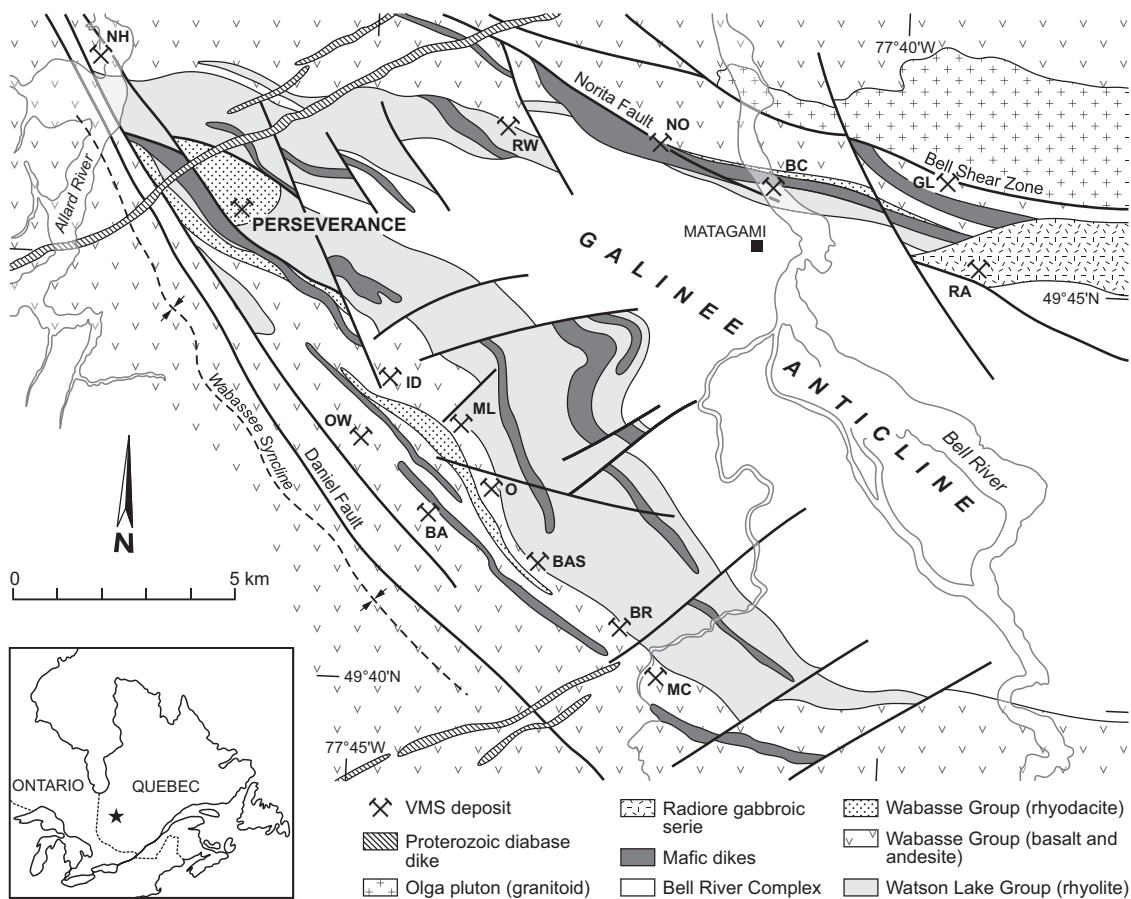


Fig. 1. Geologic map of the Matagami district (modified from Piché et al., 1993, and Pilote et al., 2011). North Flank deposits: BC = Bell Channel, GL = Garon Lake, NH = New Hosco, NO = Norita, RA = Radiore, RW = Radiore West. South Flank deposits: BA = Bell Allard, BAS = Bell Allard South, BR = Bracemac, ID = Isle Dieu, MC = McLeod, ML = Mattagami Lake, O = Orchan, OW = Orchan West.

represent a homogeneous calc-alkaline tuff resulting from the progressive deposition of andesitic ash in the water column (Genna et al., 2014). Although most of the discoveries in the district have been made at this very productive interval, new deposits are also being discovered at different stratigraphic positions, associated with different rhyolitic units and different volcano-sedimentary marker units (e.g., Upper Bracemac zone at Bracemac and St-Pat zone at McLeod; Adair, 2009; Mercier-Langevin et al., 2014).

The Wabasse Group consists of a 1.8- to 3-km-thick succession of dark pillowed tholeiitic basalts and light-colored massive to pillowed andesites (MacLean, 1984; Debrel, 2014). At least two felsic units have been recognized at the base of this mafic-dominated succession: the >200-m-thick Dumagami rhyodacite (2725.4 ± 0.7 Ma; Ross et al., 2014) and the 25- to 60-m-thick Bracemac rhyolite (2725.8 ± 0.7 Ma; Ross et al., 2014).

Both the Watson Lake and Wabasse Groups are locally intruded by late phases of the underlying Bell River Complex, a large (>5,000-m-thick) tholeiitic gabbro-anorthosite layered intrusion dated at $2724.6^{+2.5}_{-1.9}$ Ma (Mortensen, 1993). Several authors, including Maier et al. (1996), Ioannou and Spooner (2007), and Carr et al. (2008), have suggested that the Bell River Complex acted as the heat source for seawater convection and the formation of VMS deposits in the district. Geochemical similarities with the Watson Lake and Wabasse Group tholeiitic basalts suggest that these units were derived through fractionation processes of the Bell River Complex (MacGeehan and MacLean, 1980). A bulk of the Bell River Complex is interpreted as having emplaced prior to and/or during VMS formation (Maier et al., 1996, Ioannou and Spooner, 2007).

Volcanic rocks of the region have undergone greenschist facies metamorphism (Jolly, 1978) and are folded by the Galinée anticline, a broad WNW-plunging structure that separates the district into the North Flank and South Flank areas (Fig. 1). Two stages of deformation are recorded in the region, resulting from north-south convergence and the collision of the Opatica subprovince to the north (Beaudry and Gaucher, 1986; Pilote et al., 2011). The main deformation is represented by a steeply dipping, E-W-trending schistosity (S_1) in association with regional folds, including the Galinée anticline. A second phase of deformation (D_2) is documented in the North Flank of the district and is defined by a SW-NE-trending schistosity (S_2) and small-scale folds (F_2) with steep plunges to the south (Beaudry and Gaucher, 1986). The South Flank is affected by a regional NW-SE-trending high-angle reverse fault referred to as the Daniel fault, displacing the volcanic succession up to 500 m vertically (Adam et al., 1998). A generation of late transverse faults striking between $N30^\circ$ and $N45^\circ$ also crosscuts the volcanic succession along the South Flank (Fig. 1).

The North Flank of the district is characterized by an E-W-trending stratigraphy dipping steeply to the north. This area is affected by a penetrative deformation with strongly foliated and flattened rocks along numerous anastomosing shears sub-parallel to the lithologic trend. Regional metamorphism in the North Flank locally reaches middle amphibolite facies east of the Bell River (Jolly, 1978; Beaudry and Gaucher, 1986; Piché et al., 1993). Most of the VMS deposits of the North Flank

area have recorded a strong deformation with flattening and rotation of the lenses along the main schistosity (e.g., Norita; Piché et al., 1993). In contrast, the South Flank is described as weakly deformed (Piché et al., 1993; Lavallière et al., 1994; Ross et al., 2014), with variable southward to westward dips increasing from 20° in the vicinity of the Perseverance deposit to a maximum of 60° close to the Bracemac-McLeod deposit. It was previously interpreted that the deformation in this area is confined to narrow brittle-ductile shear zones with no impact on VMS deposits (Lavallière et al., 1994; Arnold, 2006).

Geology of the Perseverance Deposit

Perseverance is the northwestern-most polymetallic VMS deposit discovered in the South Flank of the Matagami mining district. The deposit consists of four distinct orebodies located within an area of 800×500 m: Equinox, Perseverance-West, Perseverance-Main, and a smaller satellite lens, Perseverance-2 (Fig. 2). The discovery results from a diamond drilling program designed to test airborne EM geophysical anomalies in an area considered to be geologically prospective (Arnold, 2006).

General stratigraphy

The four massive sulfide lenses of the Perseverance deposit occur at and below the contact between the footwall Watson rhyolite and the hanging-wall Dumagami rhyodacite (Fig. 3A, B). The orebodies are characterized by pipelike geometries entirely discordant to the host volcanic succession, which dips at an average of 20° toward the west in this area (Figs. 2, 3). This setting is in contrast with the rest of the district where the deposits are either mound shaped in a moderately dipping succession (e.g., Mattagami Lake: Roberts, 1975) or tabular shaped in a steeply dipping succession (e.g., Norita: Piché et al., 1993, and Bracemac-McLeod: Adair, 2009). Syn-volcanic structures at high angle to bedding have been suggested to control the emplacement of the orebodies (Arnold, 2006). Displacements along a series of west-northwest late brittle-ductile faults—possibly involving reactivation of early structures—such as the New Hosco fault (Figs. 2A, 3A) are interpreted to be responsible for the preservation of a structural bloc containing the near-horizontal host stratigraphy (Arnold, 2006).

Lithofacies

The Watson rhyolite constitutes the principal host unit of the four orebodies (Fig. 3A, B). Primary volcanic textures are locally preserved in the rhyolite, including hyaloclastic breccias, flow banding, and columnar jointing (Beaudry and Gaucher, 1986; Piché et al., 1993). The rhyolite varies from aphyric to porphyritic with millimeter-sized quartz and albite phenocrysts set in a groundmass of microcrystalline quartz, plagioclase, and chlorite. Characteristic centimeter-sized amygdules filled with quartz and chlorite constitute 5 to 10% of the rock volume and are locally associated with abundant spherulites.

At Perseverance, the Key Tuffite is present on top of the Watson rhyolite and immediately below the Dumagami rhyodacite of the overlying Wabasse Group. Its thickness ranges between 0.1 and ~3 m with variations occurring over

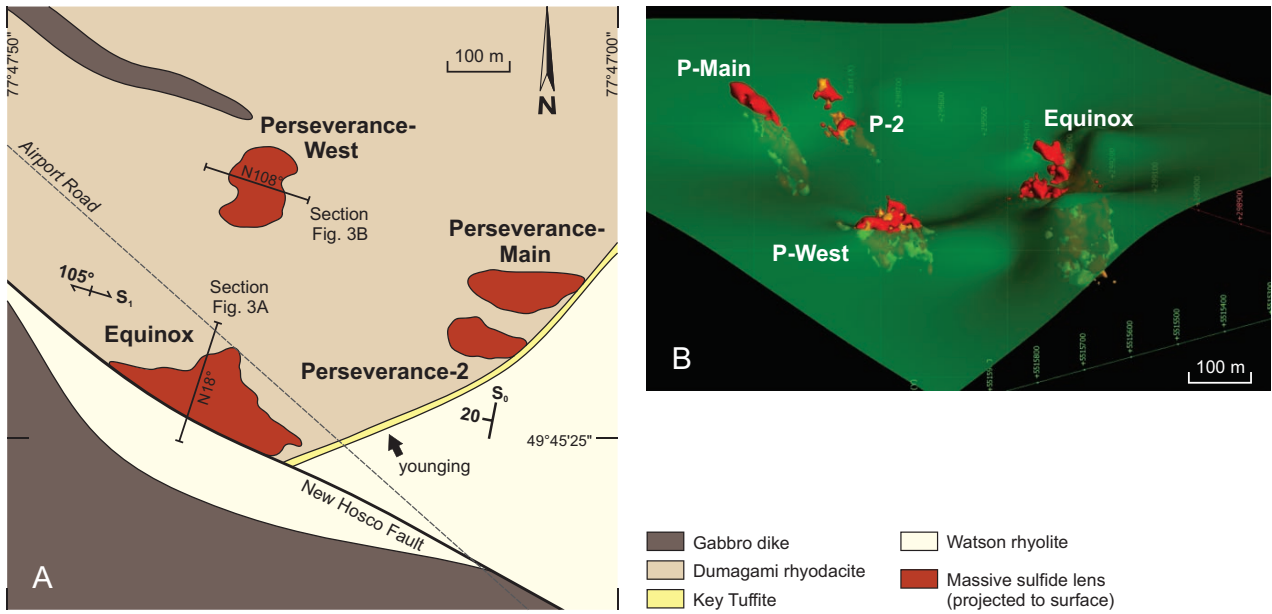


Fig. 2. Simplified geology of the Perseverance deposit. A. Surface map showing distribution of the orebodies (projected from level 130) and main lithologies. B. Three-dimensional model (looking southeast) showing the relationship between the orebodies (red) and the Key-Tuffite surface (green). Modified from unpublished Glencore Canada Corporation data.

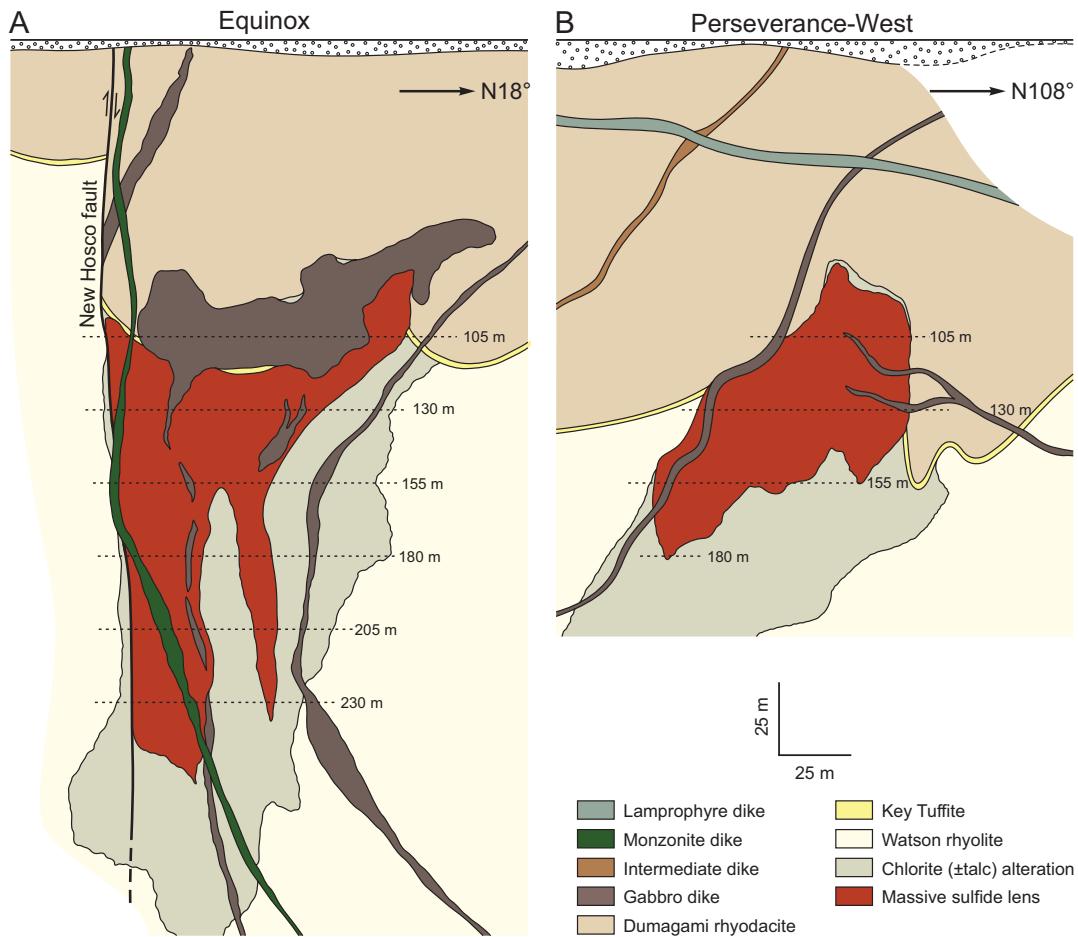


Fig. 3. Simplified geologic sections through the Equinox (A) and Perseverance-West (B) orebodies, showing the inferred schematic distribution of the principal units that host the deposit, the ore lenses (production levels are indicated) and associated chlorite alteration zones. Modified from unpublished Glencore Canada Corporation data.

short distances. The unit is commonly exposed at the upper extremity of the orebodies and generally overlies the massive sulfides (i.e., Equinox: Figs. 3A, 4A). The Key Tuffite can also be traced lower in the stratigraphy, within the upper portion of the massive sulfides. This is shown by the presence of clasts in the orebodies (Fig. 4B) and by locally highly mineralized horizons proximal (i.e., less than 10 m) to the ore (Fig. 4C). At the upper extremity of the orebodies, the unit is typically affected by a pervasive black chlorite alteration, various degrees of quartz alteration, but is devoid of mineralization (Fig. 4A). Lower in the stratigraphy, the unit displays intense alteration in chlorite (\pm quartz) in association with selective sulfide replacement along favorable layers. The Key Tuffite is almost completely devoid of sulfides several hundreds meters away from the orebodies and the hydrothermally altered area (Arnold, 2006; Genna et al., 2014). This lack of sulfides away from the deposit is unusual for the South Flank area, where it typically contains 1.5 to 2 wt % Zn as well as variable percentages of pyrite (Davidson, 1977; Liaghat and MacLean, 1992).

The overlying Wabasse Group is represented in the vicinity of the deposit by the Dumagami rhyodacite. The unit is bounded by faults to the north and to the south of the Perseverance area and its upper contact has been eroded. The Dumagami rhyodacite displays a minimal thickness of 400 m (Arnold, 2006) and constitutes the hanging wall of the four orebodies along with the Key Tuffite unit (Fig. 3). Locally however, the rhyodacite is in direct contact with the top of the orebodies and the Key Tuffite is absent (Figs. 3, 4D). Primary volcanic textures are preserved in the rhyodacite, including hyaloclastic breccias and columnar jointing. Millimeter- to centimeter-sized spherulites are locally abundant and can constitute up to half of the rock volume, as observed near the lower contact of the unit. The rhyodacitic hanging wall of the Perseverance deposit and the rhyolitic hanging wall described at Bracemac-McLeod (Adair, 2009) constitute two stratigraphic exceptions at Matagami, where mafic volcanic units typically overlay the deposits (e.g., Mattagami Lake, Isle-Dieu, and Norita).

Different generations of dikes and intrusions are present in the deposit and crosscut the volcanic succession as well as the massive sulfide orebodies. The oldest generation is characterized by a series of tonalitic dikes typically affected by chlorite alteration; one of them has a thickness reaching 30 m and occurs between the Perseverance-Main and Perseverance-2 lenses. Tholeiitic gabbro dikes constitute a second generation of intrusive rocks with thicknesses varying between a few centimeters and several tens of meters. A major tholeiitic gabbro sill subconcordant to the stratigraphy and connected with vertical feeders occurs immediately above the Equinox orebody (Fig. 3A). Tholeiitic gabbros are fine grained, massive, and typically strongly hydrothermally altered in and around the orebodies. Previous dike generations are in turn crosscut by a family of green calc-alkaline dikes of intermediate composition, typically ~1 m thick, aphyric, and variably affected by hydrothermal alteration. Two late generations of calc-alkaline monzonite and lamprophyre dikes also intrude the volcanic succession with an average thickness of 5 m and are not affected by alteration. Lamprophyre dikes generally strike northwest and have shallow northerly dips (Arnold, 2006).

Mineralization and alteration

Mineralization: The ore zones at Perseverance are dominated by Zn-Cu-rich massive sulfides with variable amounts of base metal-poor pyritic sulfides. The mineralization consists of a variety of facies, broadly identical throughout the four orebodies: (1) stringer sulfides occurring within chlorite-rich zones, (2) sphalerite- and chalcocopyrite-rich massive sulfides, (3) banded massive sulfides, (4) massive pyritic sulfides with minor sphalerite and chalcocopyrite, and (5) lenticular masses of magnetite. Stringer sulfides consist of fine- to coarse-grained pyrite with lesser chalcocopyrite and sphalerite, and constitute ~10 to 50 vol % of the rock at the base and in the periphery to the orebodies. These stringers grade into massive sulfides in the upper portion of the lenses, where pyrite, sphalerite, chalcocopyrite, varying proportions of pyrrhotite and minor galena represent up to 95 vol % of the rock. Banded sulfides consist predominantly of pyrite with varying proportions of sphalerite, chalcocopyrite, and pyrrhotite that form millimeter- to centimeter-thick bands (Fig. 4E). Magnetite occurs in varying percentages throughout the massive sulfides as disseminated, semimassive, and massive zones (Fig. 4F). The largest magnetite zone consists of a distinct 25-m-thick envelope located at the base of the Perseverance-Main orebody. The different facies are generally closely associated in space with gradual transitions from one to another, except for the lenticular masses of magnetite that have sharp contacts.

Alteration: Hydrothermal alteration is well developed in the volcanic rocks of the Perseverance deposit. Altered rocks consist predominantly of chlorite, sericite, variable proportions of talc and quartz.

The footwall Watson rhyolite is affected by a pronounced hydrothermal alteration in the vicinity of the four orebodies, increasing from weakly altered ~150 m away from the ore to intensely altered within a ~50-m inner zone. Sericite constitutes the outermost alteration and progressively transitions into black chlorite and talc in the immediate vicinity of the orebodies. The most intense alteration is characterized by a near-complete replacement of the volcanic rocks and forms visually distinct pipes around each orebody (Fig. 3). The Watson rhyolite contains poor mineralization outside these zones of intense alteration. Talc is present in variable proportions throughout the deposit and is particularly abundant in the Perseverance-West alteration halo where it forms semi- to massive zones. Talc is closely associated with chlorite and textural relationships indicate that it represents the most ore-proximal facies of the alteration halo (Fig. 4G). Quartz alteration occurs as patchy zones within the volcanic rocks and is particularly marked in and immediately around the Key Tuffite unit.

Strong hydrothermal alteration is present in the hanging-wall Dumagami rhyodacite and is dominated by black chlorite with local quartz alteration at the base of the unit. Chlorite alteration in the rhyodacite varies from patchy to pervasive with a near-complete replacement of the rock. Chlorite aggregates corresponding to the patchy alteration facies show combined recrystallization and realignment parallel to the planes of foliation (Fig. 4H).

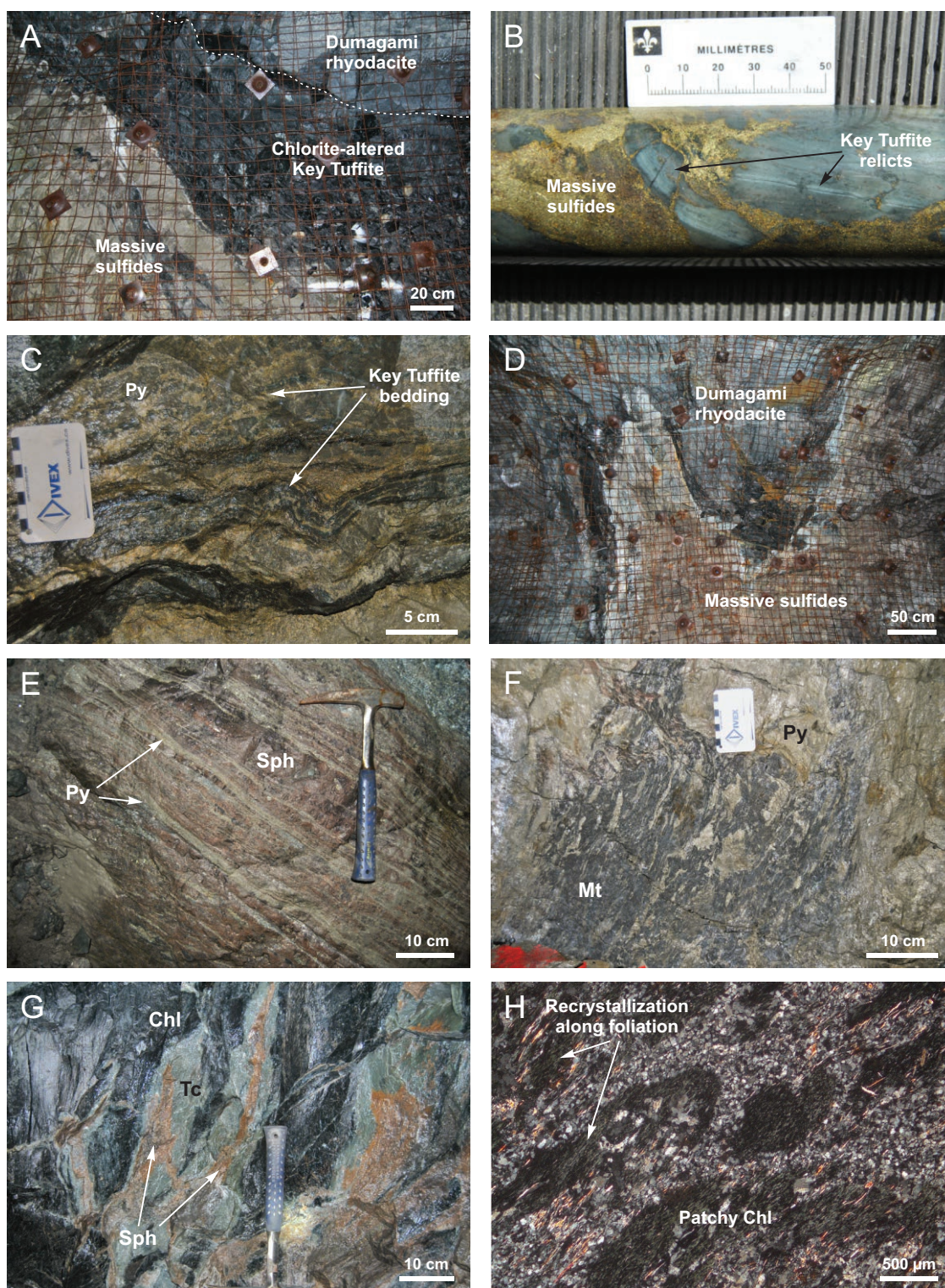


Fig. 4. A. Upper contact of Equinox overlain by the Key Tuffite and the Dumagami rhyodacite units, stope 105-EQ-25. B. Relicts of thinly bedded Key Tuffite within the upper portion of the Perseverance-West orebody, drill hole PER-00-20. C. Intricate sulfide replacement of the Key Tuffite laminations in proximity to the Equinox orebody, stope 130-EQ-25. D. Upper portion of the massive sulfides in direct contact with the hanging-wall Dumagami rhyodacite, stope 105-PW-16. E. Plan view of typical sphalerite-rich banded ore, stope 105-EQ-20. F. Magnetite-rich facies in contact with massive pyritic ore, stope 105-EQ-18. G. Proximal talc alteration in close spatial relationship with sphalerite veins and chlorite-rich zones, stope 105-PW-18. H. Patchy hydrothermal chlorite showing recrystallization and realignment parallel to foliation (photomicrograph in transmitted light, drill hole PER-00-20). Abbreviations: Chl = chlorite, Mt = magnetite, Py = pyrite, Sph = sphalerite, Tc = talc; EQ = Equinox, PW = Perseverance-West.

Metal zonation

Metal zonation of the Perseverance orebodies is illustrated in Figure 5 and corresponds to the geologic sections of Figure 3. The sections cut the thickest zones of the Equinox and Perseverance-West orebodies and are representative of the metal distribution within these lenses. Distribution of Zn at Equinox (Fig. 5A) is associated with increasing grades toward

the upper section of the lens, with highest values (reaching 38.7 wt % Zn) occurring immediately below the hanging-wall contact. At Perseverance-West, Zn grades are higher in the outermost portions of the lens, whereas relatively lower values occur in the core and uppermost portions of the orebody. Copper distributions of the Equinox and Perseverance-West orebodies (Fig. 5B) are comparably more dispersed than Zn.

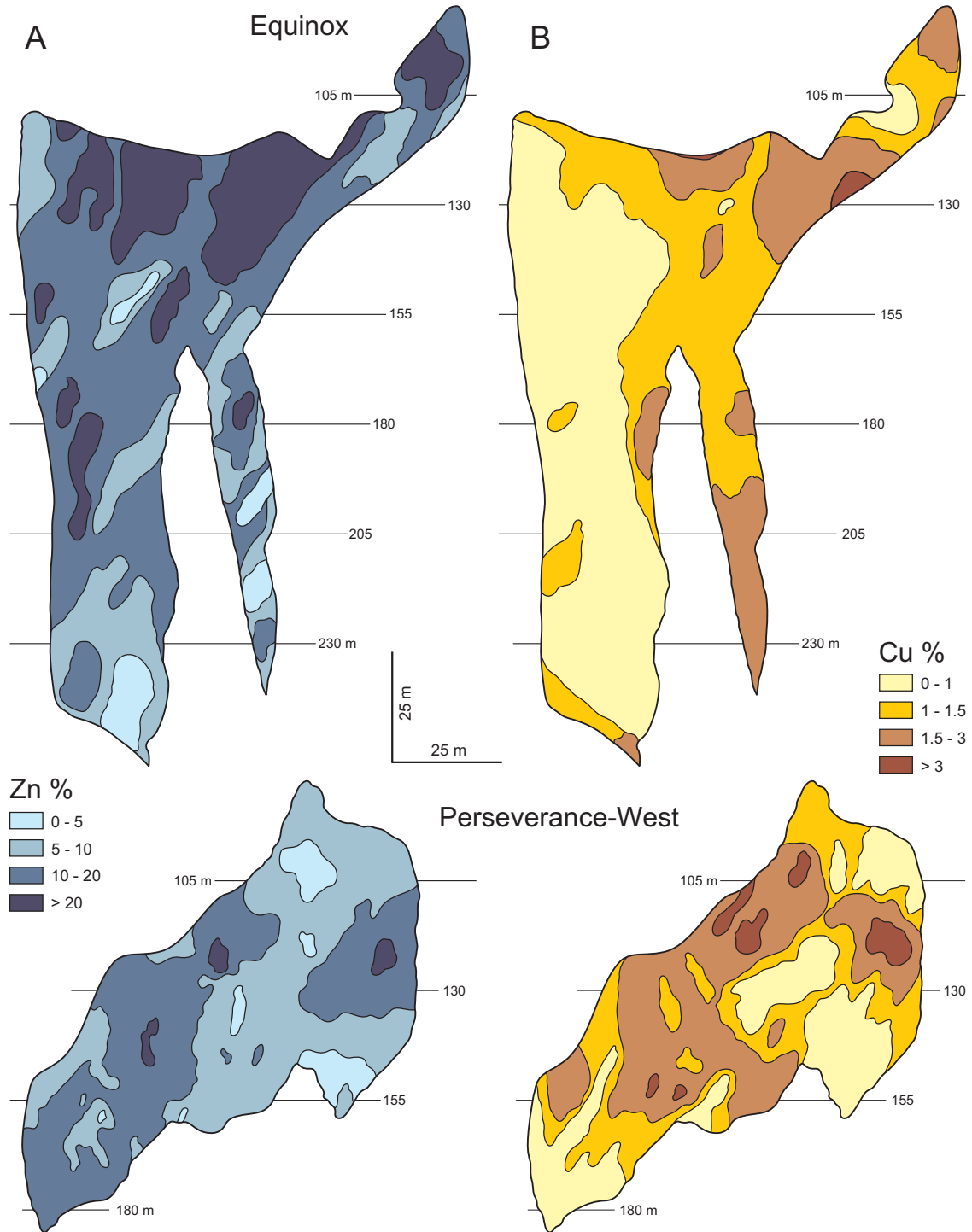


Fig. 5. Zinc and Cu distributions of the Equinox (looking west) and Perseverance-West (looking north) orebodies. Vertical sections from unpublished Glencore Canada Corporation block model resource estimate.

The northern half of the Equinox orebody displays higher Cu grades (up to 3.1 wt % Cu) than its southern half, whereas no vertical zonation of Cu exists in the lens. At Perseverance-West, higher Cu grades are located in the central part and in the central lateral margins of the orebody (reaching 4.7 wt % Cu), with comparatively lower values at its upper and lower extremities.

Sampling and Analytical Methods

Data used for the alteration geochemistry study are supplemented by 2,807 whole-rock geochemical analyses from Glencore Canada Corporation, corresponding to 231 exploration and delineation drill holes of the Perseverance area. Analyses were performed at the Chimitec commercial laboratory in Vancouver, British Columbia, for major element oxides and trace elements using X-ray fluorescence. Precision and accuracy of these data were validated to be robust using the systematic insertion of sample replicates and procedural blanks. Thirty-nine samples of the various lithologies were also collected underground and analyzed for reference by ALS Minerals at Val d'Or, Quebec, using fusion ICP-AES for major elements and fusion ICP-MS for trace elements. Statistical analysis indicates that the two whole-rock datasets are homogeneous and compatible, so they were combined for interpretation of the hydrothermal alteration geochemistry.

Mass-balance calculations were carried out on a total of 1,711 whole-rock analyses from the footwall and hanging-wall rocks. Gains and losses of mobile elements are based on the concentration or dilution of an immobile element monitor (Gresens, 1967; Barrett and MacLean, 1994). Hydrothermal alteration at Perseverance had no influence on TiO₂ concentrations and this element is used as immobile monitor. Mass changes of mobile elements in altered samples of the two units are evaluated by comparison with their respective precursor composition in a single precursor system—an average of two least altered samples is used as the precursor composition for each unit. The absolute mass change (expressed in g/100 g) for each component is calculated using the following formula:

$$\text{Mass change} = \left(\frac{\text{TiO}_2 \text{ precursor}}{\text{TiO}_2 \text{ altered}} \times \% \text{element altered} \right) - \% \text{element precursor}.$$

This approach assumes no change in during hydrothermal alteration. Absolute mass changes were evaluated separately in the two main host volcanic units (i.e., footwall rhyolite and hanging-wall rhyodacite) for principal major oxides. Mapping of the results on two plans was achieved using samples coordinates and an inverse distance weighting method on Mapinfo-Discover.

Representations of Cu and Zn distributions in the orebodies were obtained from the block model resource estimate of the Perseverance feasibility study (Arnold, 2006). Three-dimensional block models were constructed by ordinary kriging interpolations for the Equinox, Perseverance-Main, and Perseverance-West orebodies. The models were constrained with 7,966 base metal assays at 1-m intervals performed at the Chimitec commercial laboratory in Vancouver, British Columbia, by atomic absorption spectroscopy (AAS) for Zn, Cu, Pb, and Ag. The sections presented in this study correspond to 2.5-m-thick slices of the block model.

Alteration Geochemistry

The analysis of hydrothermal alteration zones provides valuable information on the processes associated with the formation of VMS deposits (Riverin and Hodgson, 1980; Gemmill and Fulton, 2001; Gemmill and Herrmann, 2001; Franklin et al., 2005). In contrast to footwall alteration zones, the recognition of hanging-wall alteration is more difficult as the mineralogical, compositional, and textural changes are commonly less pronounced (Doyle and Allen, 2003; Franklin et al., 2005). In this section, whole-rock compositions of both the footwall and hanging-wall zones will be used to establish the relationships between hydrothermal alteration and the massive sulfide orebodies.

Lithochemistry

The volcanic and intrusive rocks of the Perseverance area are plotted in a TiO₂ versus Zr diagram (Fig. 6A) to define the chemical homogeneity of the units as well as their alteration lines. TiO₂ and Zr are used for their ability to remain immobile during hydrothermal alteration and metamorphism (MacLean and Kranidiotis, 1987; MacLean, 1990). The diagram shows linear trends of correlated points with positive slopes for all lithologies, which confirm the immobility of the two elements. During hydrothermal alteration, mass changes of mobile components influence the concentration of immobile elements. These variations generate a spread of data along the linear trend with net mass gains moving the rocks toward the origin and net mass losses moving them in the opposite direction (MacLean and Barrett, 1993). Both the footwall Watson rhyolite and the hanging-wall Dumagami rhyodacite have low TiO₂/Zr ratios and their respective alteration lines illustrate significant mass changes (Fig. 6A).

Alteration indexes

Two alteration indexes have been tested on the footwall and hanging-wall geochemical data sets (Fig. 6B). The alteration index (AI, Ishikawa et al., 1976) relates to the replacement of plagioclase by sericite and chlorite during hydrothermal alteration and the chlorite-carbonate-pyrite index (CCPI, Large et al., 2001) measures the degree of chlorite, pyrite, and/or carbonate alteration. A dominant fraction of the samples plots well outside the least altered box, indicating significant geochemical changes during hydrothermal alteration of the host volcanic rocks. A clear trend of chlorite ± sericite ± pyrite alteration typical of proximal VMS footwall alteration can be outlined for both the footwall and hanging-wall rocks. Alteration index values range from 14.1 to 99.1 and CCPI index values vary from 29.8 to 99.9 for the hanging-wall Dumagami rhyodacite. Sericite, epidote, carbonate, and K-feldspar alteration trends are absent in the immediate vicinity of the deposit.

Mass-balance calculations

The technique of mass-balance calculations is used to quantify the amounts of individual elements added to or removed from the rocks as a result of hydrothermal alteration (Gresens, 1967; Grant, 1986; MacLean, 1990; Barrett and MacLean, 1994). Absolute mass gains and losses are evaluated in the footwall and hanging-wall rocks by comparison with a single precursor composition for each unit (see "Analytical Methods" for

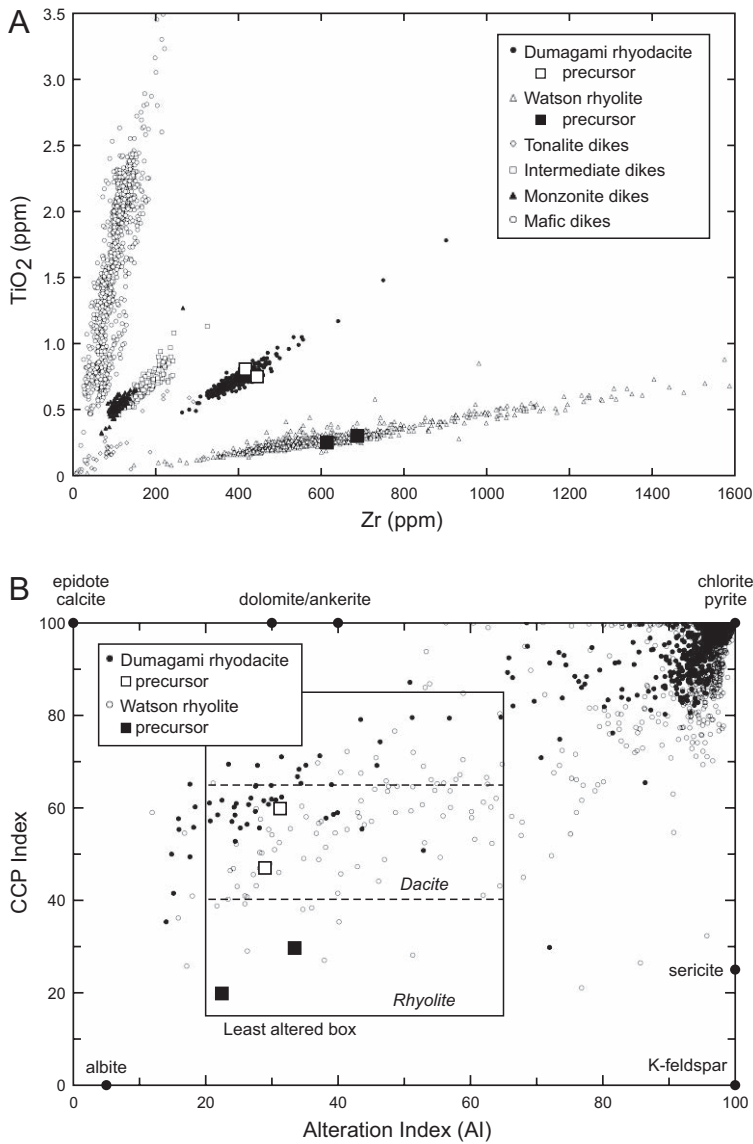


Fig. 6. Discrimination diagrams for the Perseverance volcanic rocks. A. TiO₂-Zr plot, showing the internal homogeneity of the various lithologies and their chemical trends corresponding to mass changes. B. Alteration index (AI)-chlorite-carbonate-pyrite index (CCPI) box plot, showing hydrothermal alteration trends in the immediate vicinity of the deposit (least altered box for felsic units from Large et al., 2001). AI = 100(MgO + K₂O)/(MgO + K₂O + Na₂O + CaO), CCPI = 100(FeO + MgO)/(FeO + MgO + Na₂O + K₂O).

calculation details). Least altered samples were chosen from drill cores intersecting the volcanic rocks tens to hundreds of meters away from the alteration plumes and show no visible effect of hydrothermal alteration on hand samples and from thin-section observations. Mass changes are calculated for 1,066 samples of the footwall rhyolite and 645 samples of the hanging-wall rhyodacite. Average geochemical compositions of the two units and their respective precursor compositions are listed in Table 1.

Mapping of mass changes at Perseverance enables visualization of the geometric relationships between the massive sulfide orebodies and hydrothermal alteration in the host volcanic succession. Results from mass-balance calculations are presented in two plans corresponding to the footwall and hanging wall, respectively (Fig. 7). The footwall plan encompasses all analyses of the Watson rhyolite and the hanging-wall plan includes all analyses of the Dumagami rhyodacite; both involve vertical projections of the samples. Positions of the samples used for whole-rock analysis and mass-balance

calculations are shown in Figure 7A and B relative to the location of the orebodies, whereas Figure 7C to H illustrates the corresponding absolute mass changes for representative major mobile elements.

Predominant mass changes are identified in both the foot-wall and hanging-wall rocks for the major oxides MgO, K₂O, and Na₂O. Major mass changes in MgO are indicated in the footwall Watson rhyolite (Fig. 7C) with gains greater than 10/100 g and highest values attaining ~49/100 g. Halos corresponding to these mass gains are closely correlated with the location of the four orebodies and have dimensions of up to ~400 m in diameter (i.e., Perseverance-Main). Strong mass gains in MgO are also present in the hanging-wall Dumagami rhyodacite (Fig. 7D) and similarly exceed 10/100 g with maximum values at ~17/100 g. Mass gain halos in the hanging-wall rocks are also correlated with the position of the orebodies but are spatially less developed than in the footwall (i.e., <200 m at Perseverance-Main). Geochemical data show that mass gains in MgO are persistent up to 70 m above the orebodies in the

Table 1. Geochemical Compositions of the Volcanic Units and Their Respective Precursors

Facies Sample	Altered footwall		Precursors footwall		Altered hanging wall		Precursors hanging wall	
	<i>n</i> = 1,066		81822M	79903M	<i>n</i> = 645		862161	64803M
	Mean	Std. dev.			Mean	Std. dev.		
Major oxides ¹ (%)								
SiO ₂	71.82	13.15	75.66	78	69.85	4.94	74.4	72.23
TiO ₂	0.25	0.09	0.29	0.25	0.72	0.08	0.74	0.82
Al ₂ O ₃	9.84	3.26	11.07	9.54	10.60	1.2	11.58	10.85
Fe ₂ O ₃	5.65	3.95	2.11	1.22	6.10	2.16	3.62	5.98
MnO	0.03	0.04	0.03	0.03	0.03	0.03	0.07	0.06
MgO	6.92	6.20	0.82	0.28	6.87	3.08	0.98	1.41
CaO	0.06	0.78	0.88	1.59	0.19	0.73	1.69	1.28
Na ₂ O	0.09	0.96	4.57	4.3	0.12	1.01	3.63	3.67
K ₂ O	0.17	0.81	1.92	1.4	0.36	0.47	1.18	0.83
P ₂ O ₅	0.03	0.06	0.05	0.03	0.13	0.26	0.14	0.16
LOI	3.83	2.30	1.2	1.19	4.07	1.62	1.89	1.92
Total	99.20	0.55	98.64	98.1	99.34	0.47	99.98	99.3
Ratios and alteration indices								
Al ₂ O ₃ /TiO ₂	38.83	3.67	38.17	38.16	14.59	0.74	15.65	13.23
TiO ₂ /Zr	4.33	0.49	4.13	4.11	18.28	0.68	16.41	18.94
Zr/Y	4.16	1.49	3.99	4.90	3.53	0.49	3.5	2.5
AI ²	97.68	5.43	33.46	22.19	95.34	18.82	28.88	31.15
CCPI ³	98.14	15.88	29.52	19.47	95.41	10.98	46.84	60.15

¹ Major and trace elements performed by X-ray fluorescence

² Alteration index from Ishikawa et al. (1976)

³ Chlorite-carbonate-pyrite index from Large et al. (2001)

hanging wall. Drill core observations and detailed mapping of the volcanic rocks indicate that the geochemical anomalies in MgO correspond to chlorite-rich zones and to variable proportions of talc.

Less intense mass changes are recorded for K₂O in the footwall Watson rhyolite with losses on the order of $-2.1/+100$ g (Fig. 7E). Mass losses in K₂O are also present in the hanging-wall rocks with lower values reaching $-1.2/+100$ g (Fig. 7F). The depletion halos related to K₂O match the geometries and dimensions of MgO enrichments in both the footwall and hanging-wall rocks, showing an opposite behavior for these two components. Small mass losses are also indicated for Na₂O in the footwall rocks with values reaching $-4/+100$ g (Fig. 7G) and in the hanging-wall rocks with similar depletions (Fig. 7H). Strongest depletions in Na₂O are correlated with the position of the orebodies and mass losses are still significant (on the order of $-3/+100$ g) several hundreds of meters away from the ore in the footwall. Depletion halos for Na₂O in the hanging-wall rocks are comparably more constrained to the immediate proximity of the orebodies, as illustrated at Perseverance-West and Perseverance-Main. Depletions in alkali components are extensive when taking into account their low initial concentrations before hydrothermal alteration (see precursor compositions in Table 1). Petrographic observations and interelement relationships indicate that mass losses in K₂O and Na₂O result from the breakdown of feldspar during chloritization.

Structural Geology

The four Perseverance orebodies and their enclosing volcanic rocks are affected by a significant structural overprint related

to postdepositional deformation. The mechanisms of deformation and their intensity are emphasized by the physical behavior of the sulfide assemblage and by the modification of original textures in the volcanic rocks.

Host rocks

A penetrative schistosity is present in various outcrops of the Watson rhyolite located several hundreds of meters away from the Perseverance deposit; the fabric typically crosscuts primary structures of the rhyolite, such as massive flow lobes (Fig. 9A). This schistosity is particularly marked in the immediate vicinity of the deposit where hydrothermal alteration is developed. Measurements of the fabric within the proximal host rocks indicate a near-vertical schistosity oriented at N105° (Fig. 8A). This value corresponds to the direction of S₁ and to the regional deformation stage D₁. Mineral stretching lineations L₁ present within the foliation planes have a moderate to steep plunge to the west (Fig. 8A).

Original bedding (S₀) around the deposit is indicated by depositional laminations within the Key Tuffite unit. Drill core information in the South Flank indicates that the stratigraphy dips to the west, with a value of $\sim 20^\circ$ around Perseverance (Arnold, 2006). The Key Tuffite locally displays steeper dips and is affected by numerous folds within a radius of <100 m from the orebodies. These folds are generally meter scale, ranging from open to isoclinal, and the measurement of their orientations indicates an axial plane F_{KT} that parallels the regional schistosity S₁ at N110° (Fig. 8A, B). The Key Tuffite is also deformed into folds of higher amplitude, as observed at Perseverance-West where a >100 -m-wide antiform surrounds the orebody (Fig. 3B). Based on underground observations,

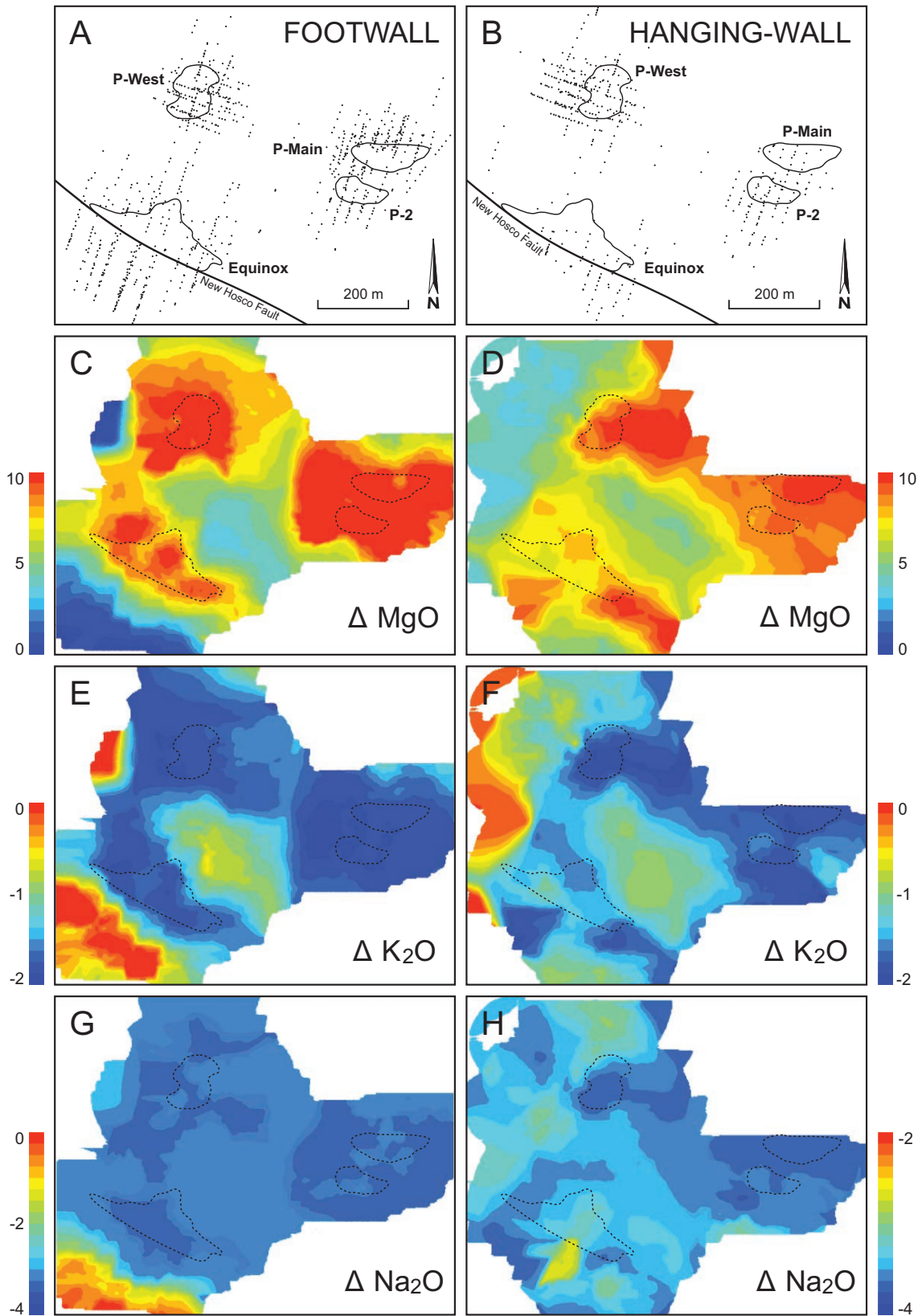


Fig. 7. Plan view showing the relationship between absolute mass changes (in g/100 g) of mobile major elements and the location of the orebodies at Perseverance. A. Projected distribution of the footwall Watson rhyolite samples. B. Projected distribution of the hanging-wall Dumagami rhyodacite samples. C. and D. Mass changes in MgO. E. and F. Mass changes in K₂O. G. and H. Mass changes in Na₂O.

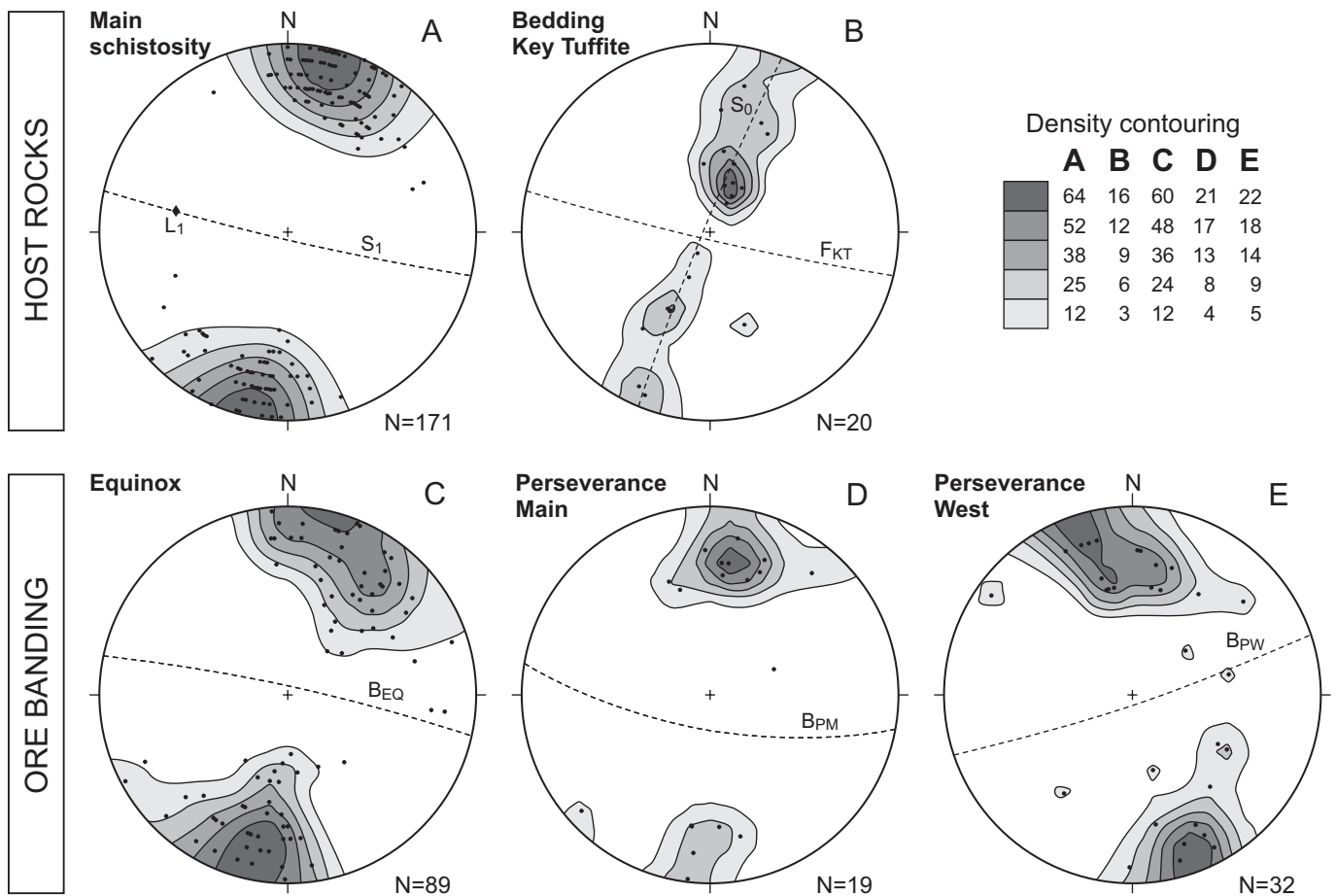


Fig. 8. Lower hemisphere equal-area projection of measured fabrics in host rocks vs. ore envelopes. A. Main schistosity (S_1) measured in moderately to strongly altered volcanic host rocks. B. Average axial plane (F_{KT}) of folds developed in the Key Tuffite unit. C. D. and E. Average attitude of the banded texture in the Equinox (B_{EQ}), Perseverance-Main (B_{PM}), and Perseverance-West (B_{PW}) orebodies.

the folds developed in the Key Tuffite increase in intensity where intense chlorite alteration is present, thus suggesting a spatial correlation between alteration and deformation (Fig. 9B).

Massive sulfide structures

Most of the orebodies at Perseverance trend parallel to each other and display a prevailing west-northwest direction (Fig. 2). This is the case for Equinox, Perseverance-Main, and Perseverance-2, where this orientation corresponds to the longest axes of the lenses (i.e., respectively 175, 135, and 60 m). The Perseverance-West orebody has a more irregular shape and only local zones at depth parallel the direction of alignment. The dominant orientation of the orebodies observed at Perseverance correlates with the direction of the regional schistosity S_1 at $N105^\circ$. The four lenses also have moderate to steep plunges toward the northwest, corresponding to the attitude of mineral stretching lineations recorded in the volcanic host rocks.

A distinct mineralogical banding is developed in the four massive sulfide orebodies, typically characterized by millimeter- to centimeter-thick monomineral bands of pyrite alternating with sphalerite and lesser amounts of chalcopyrite,

pyrrhotite, or magnetite (Fig. 4E). The mineralogical banding is recognized at all stratigraphic levels where the semi- and massive ore facies are present. The banded texture is favorably developed within the sphalerite-rich zones and progressively disappears into the massive pyrite ore facies. Mineralogical bands form subvertical planes entirely discordant to the sub-horizontal bedding of the volcanic succession. Attitudes of the banding planes were measured in the three largest orebodies and recorded in stereograms (Fig. 8). Similar orientations at $N110^\circ$ are indicated for the Equinox and Perseverance-Main lenses (Fig 8C, D) and match the attitude of the regional schistosity S_1 . At Perseverance-West, the orientation of mineralogical banding differs slightly with an average direction at $N80^\circ$ (Fig 8E). This value deviates from the orientation of the main fabric in the South Flank of the district but corresponds to the direction of the fabric S_2 developed at $\sim N75^\circ$ in the North Flank; Perseverance-West is the nearest orebody to this area relative to the rest of the deposit.

The banded ore is locally associated to ovoidal-elongate structures that parallel and interrupt the banding. These centimeter- to meter-wide structures are composed of fragments ranging from single crystals to larger clasts and show evidence of internal rotations (Fig. 9C). The brecciated rock

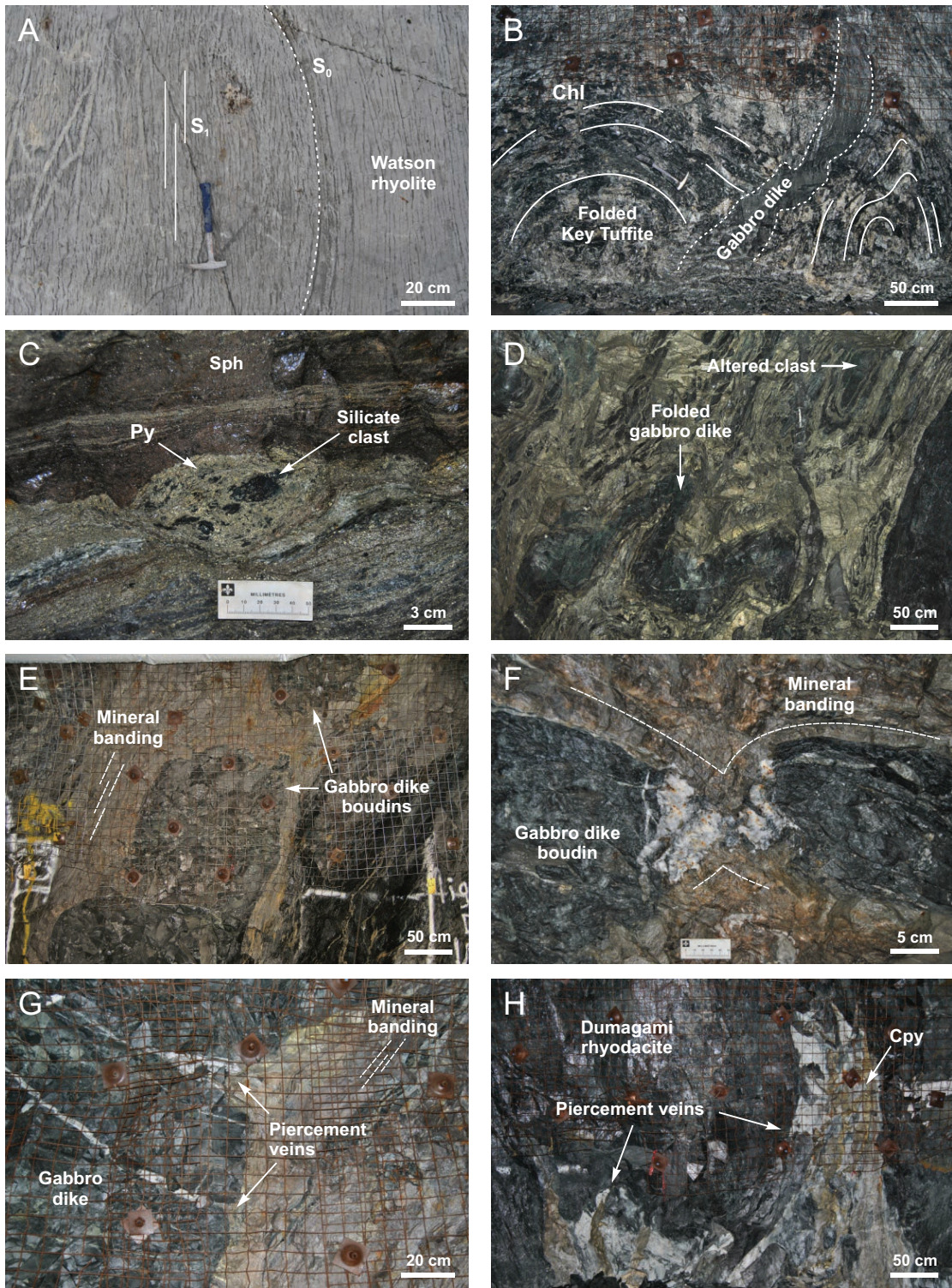


Fig. 9. A. Penetrative schistosity S_1 crosscutting lobate flows of the Watson rhyolite several hundred meters away from the deposit. B. Open to isoclinal folds developed in the Key Tuffite where intense ore-proximal chlorite alteration is recorded, stope 105-P2-01. C. Plan view of a durchbewegung structure with pyrite and silicate fragments, showing internal rotations in a matrix of banded pyrite-chalcopyrite ore, stope 105-EQ-18. D. Section view of a gabbro dike affected by isoclinal folding in massive pyrite-sphalerite ore, stope 130-EQ-25. E. Gabbro dike affected by boudinage parallel to the direction of the mineralogical banding, stope 130-EQ-18. F. Plan view of a boudinaged gabbro dike associated with apparent flow of the ductile sulfide material. G. Piercement veins developed at the interface between a dike of gabbro and massive sulfides, stope 105-EQ-18. H. Piercement vein dominantly composed of chalcopyrite at the upper extremity of the Perseverance-West ore-body, stope 105-PW-16. Abbreviations: Chl = chlorite, Cpy = chalcopyrite, Py = pyrite, Sph = sphalerite; EQ = Equinox, P2 = Perseverance-2, PW = Perseverance-West.

is typically composed of pyrite and magnetite, with variable proportions of silicate material including altered fragments of rhyolite and dikes. Apparent contrasts of rheology are illustrated between the assemblages formed by strong materials (i.e., pyrite, magnetite, and silicate rocks) and the surrounding matrix characterized by relatively weaker components of the banded ore (i.e., sphalerite, chalcopyrite, and pyrrhotite). These structures show some similarities with the “durchbewegung” texture described by Vokes (1976) and Marshall and Gilligan (1989) in metamorphosed massive sulfide deposits of the Norwegian Caledonides.

The abundant tholeiitic abbro dikes crosscutting the ore are rarely continuous and are typically intensely deformed. They are either affected by folding, boudinage, or by a combination of both. Folding is generally displayed in centimeter- to meter-thick dikes that crosscut the ore at subhorizontal attitudes. These folds are generally tight to isoclinal and are consistent with an apparent shortening of 40% (Fig. 9D). Deformation by boudinage affects a large number of gabbroic dikes in the massive sulfides regardless their thickness. The boudins are preferentially developed in dikes with subvertical attitudes and display an elongation that systematically parallels the planes of banding (Fig. 9E). Boudinage occurs both vertically and horizontally within the planes of banding, indicating stretching in two directions (Fig. 9F). Rounded boudins typically occur in the banded pyrite-sphalerite ore, whereas angular-shaped boudins are developed into the massive pyrite ore, showing competency contrasts induced by different host ore mineralogies.

The zones of separation between boudins are commonly associated with an apparent flow of the ductile sulfide material (Fig. 9F). In an early stage of the process, the ductile sulfide material forms incisions into more competent lithologies and quartz veins typically mark their extremities (Fig. 9G). These centimeter- to meter-long penetrative structures, referred to as piercement veins, are also frequent along the upper extremity of the orebodies at Perseverance (Fig. 9H). Piercement veins reflect layer-parallel or layer-oblique (shallow-angle) contraction of an interface separating materials with contrasts of competency and imply failure by pure extension or extensional brittle shear (Marshall and Gilligan, 1989). They constitute a characteristic deformation feature of massive sulfide deposits (Gilligan and Marshall, 1987; Duuring et al., 2007).

Mineral fabrics

The fabrics of sulfide ores at Perseverance reflect processes related to metamorphism, as indicated by changes in the form of minerals, producing metablastic textures and changes in grain size. In the different ore facies, pyrite typically occurs as fine-grained crystals with sizes ranging from 100 μm to less than 1 mm in diameter (Fig. 10A). A generation of coarse (>2 mm) pyrite crystals is also developed along distinct planes of the banded ore facies and within the massive pyrite-sphalerite ore, locally occurring as large (up to 40 mm) porphyroblasts (Fig. 10B). Pyrite aggregates commonly form mosaics of roughly equant grains with 120° dihedral angles at triple-junction points (Fig. 10A). Individual metablasts and

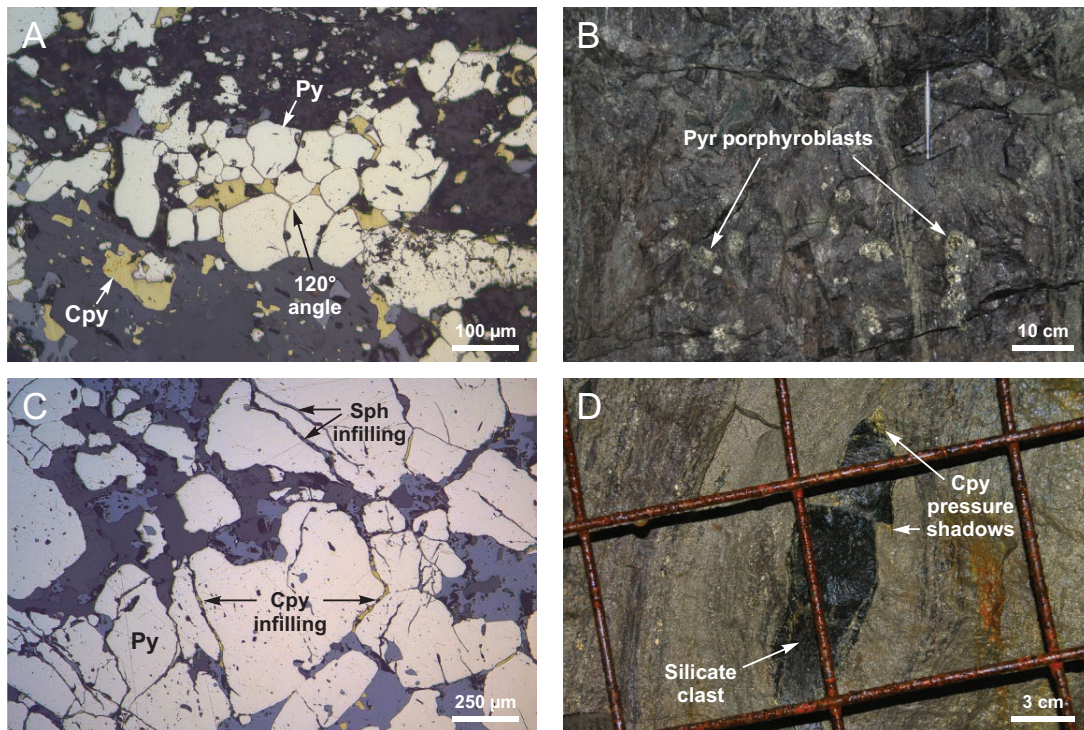


Fig. 10. A. Equidimensional pyrite grains displaying triple junctions with 120° dihedral angles, photomicrograph in reflected light, stope 105-EQ-18. B. Centimetric pyrite porphyroblasts developed within a zone of massive sphalerite, stope 105-EQ-23. C. Highly fractured pyrite grains filled by chalcopyrite and sphalerite, photomicrograph in reflected light, 105-EQ-18. D. Chalcopyrite pressure shadows developed at the extremities of a boudinaged silicate clast in the banded ore facies. Abbreviations as in Figure 9 caption.

pyrite-rich aggregates are also commonly affected by intense brittle deformation and broken by conjugate fractures (Fig. 10C). Subhedral magnetite grains in the ores are either undeformed or fractured in a brittle manner, indicating that they acted as high-strength inclusions in weaker and more ductile matrix sulfides (McQueen, 1987).

Modifications are also recorded in the distribution of the various mineral phases within the ore assemblage. Triple junction boundaries developed within pyrite aggregates and highly fractured individual pyrite metablasts are typically filled with variable proportions of chalcopyrite, pyrrhotite, and sphalerite (Fig. 10A, C). In the massive ores with high sphalerite content, chalcopyrite appears to favorably fill pyrite fractures rather than the outer edges of pyrite grains (Fig. 10C). Chalcopyrite is also typically present at the extremities of pyrite porphyroblasts, magnetite aggregates, and silicate inclusions, where it forms pressure shadows along the direction of banding (Fig. 10D). In places where folding is observed in the ore, chalcopyrite shows a systematic enrichment in hinge zones relative to other sulfides; such remobilization is also observed in association with piercement structures (Fig. 9H).

Discussion

Evidence for seafloor replacement

Previous authors (Roberts, 1975; Piché et al., 1993; Lavallière et al., 1994) proposed an exhalative model for massive sulfide deposition in the Matagami district with the formation of mound-shaped lenses in a seafloor environment. This model is mainly based on the spatial relationship between mineralized zones and the Key Tuffite in the volcanic succession, and on the interpretation that the unit constitutes a seafloor chemical precipitate genetically related to the ore (Davidson, 1977; Liaghat and MacLean, 1992).

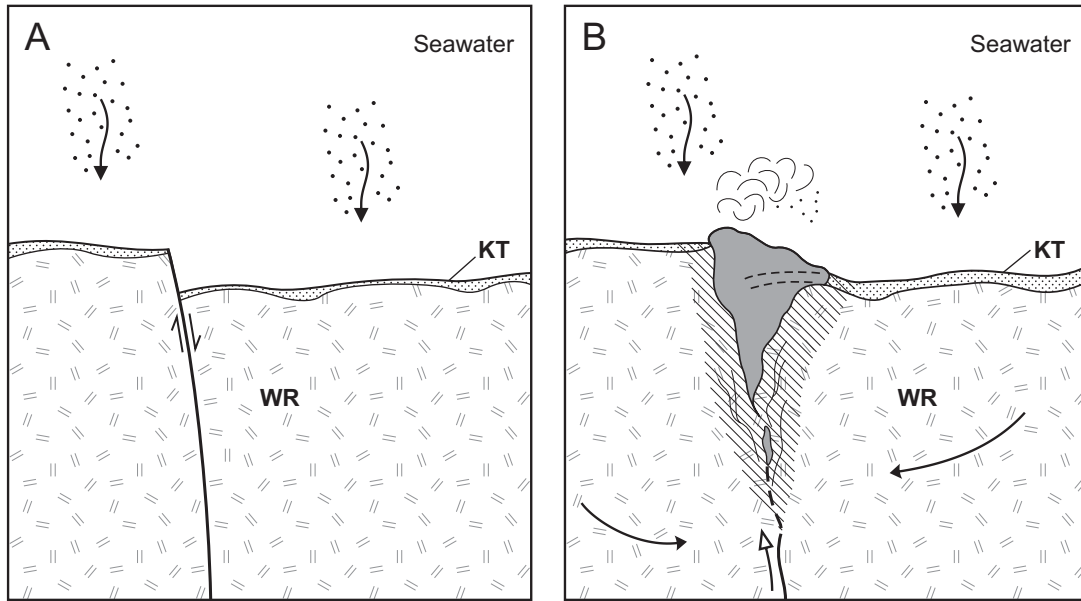
At Perseverance, the ore lenses occur on the same stratigraphic level at the interface between the Watson rhyolite and the Dumagami rhyodacite, in close association with the Key Tuffite stratigraphic marker. This lithologic setting is analogous to other deposits in the district. However, the presence of four orebodies with pipelike geometries discordant to the volcanic succession and dominantly hosted in the footwall unit is atypical. The reconstruction of primary contact relationships between the Key Tuffite and the ore is complicated at Perseverance by lateral variations in thickness and by postdepositional deformation. Variable proportions of barren Key Tuffite generally overlay the massive sulfide lenses with well-defined contacts, indicating a deposition that postdates the mineralizing event. Additionally, the presence of Key Tuffite relicts within the uppermost section of the lenses and evidence for gradational sulfide replacement within this lithofacies suggest that the mineralizing event postdates the lowermost portion of the unit. These relationships indicate that the mineralizing episode is only partially synchronous with the deposition of the Key Tuffite at Perseverance. Such interpretation is in agreement with the conclusions of Genna et al. (2014) who showed that the unit corresponds to a homogeneous calc-alkaline andesitic tuff progressively deposited in the water column, rather than an exhalite. The onset of hydrothermal activity and ore deposition at Perseverance probably started when slow tuffaceous sedimentation was already ongoing on

the seafloor (Fig. 11A, B). Such environment, characterized by a relative quiescence in the volcanic activity, was likely favorable for efficient ore accumulation and massive sulfide growth.

Most of the ore at Perseverance occurs stratigraphically below the Key Tuffite unit and is predominantly hosted (i.e., several hundred meters) within the footwall Watson rhyolite. The pipelike-shaped lenses display gradual transitions from stringer to massive sulfides and are entirely enveloped by distinctive alteration halos; such relationship most likely represents a primary characteristic of the deposit. This framework suggests that the orebodies formed dominantly by replacement of the footwall rhyolite in a subseafloor setting, during deposition of the Key Tuffite. Subseafloor replacement was most likely enhanced by the structural porosity of steep synvolcanic structures marked by the vertical chloritic (\pm talc) feeder pipes and by the presence of brecciated zones at the top of the Watson rhyolite. Upward migration of hydrothermal fluids was controlled by the permeability of the conduits, where simultaneous downward infiltration of seawater caused mixing, cooling, and sulfide deposition in a subseafloor setting (Fig. 11B; Piercey et al., 2014). The position at which hydrothermal fluids interacted with the overlying water column assumably changed with time, inducing sulfide accumulation at various depths below the seafloor. The four orebodies constituting the Perseverance deposit also suggest that different permeable zones existed in the footwall rocks, possibly related to a cluster of synvolcanic faults. This is in agreement with the interpretation of Arnold (2006) that the volcanic block hosting Perseverance corresponds to a grabenlike structure, with the Equinox orebody occurring immediately to the east of a normal inward-dipping fault. The unusual lack of sulfides in the Key Tuffite tens to hundreds of meters away from the deposit is coherent with a focused discharge of ascending fluids at the seafloor and concurrent subseafloor replacement. It is inferred that very little lateral flow migrated parallel to strata at Perseverance due to structural controls promoting upward movements of hydrothermal fluids.

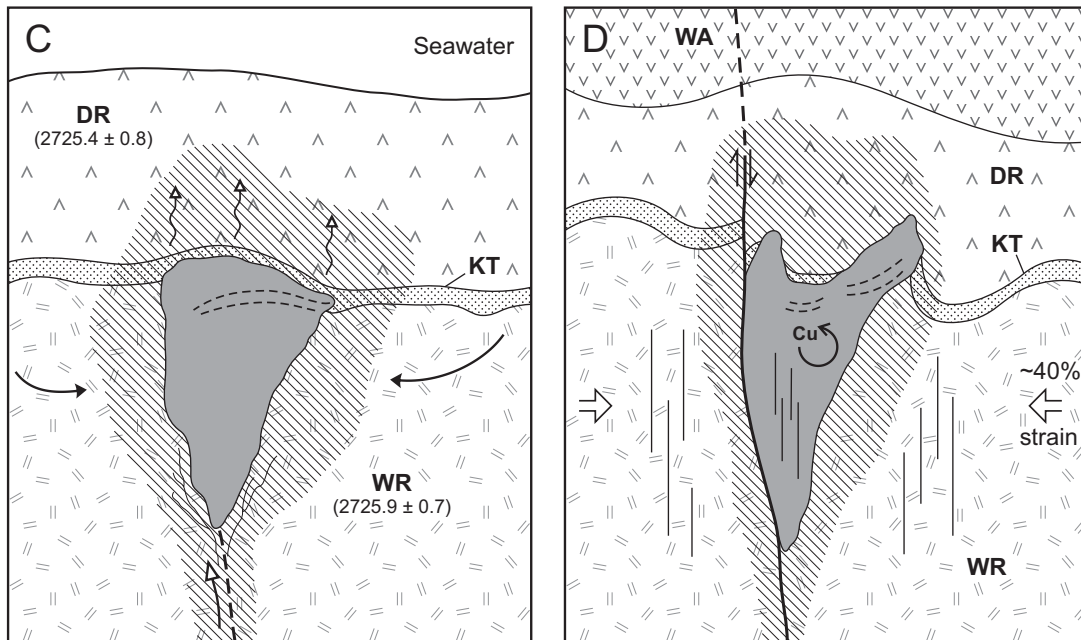
Although generally overlain by a younger and barren portion of the Key Tuffite, the upper extremities of the four orebodies are locally in direct contact with the hanging-wall Dumagami rhyodacite. The contacts with the rhyodacite are invariably sharp rather than gradational and this setting is unlikely to be caused by replacement of the unit (Doyle and Allen, 2003). It is interpreted that the orebodies were emplaced before deposition of the hanging wall and were remobilized to different degrees into this unit during deformation (see following section).

Hydrothermal alteration at Perseverance extends into the hanging-wall rocks, affecting both the Dumagami rhyodacite and the upper portion of the Key Tuffite. Hanging-wall alteration is recorded up to several tens of meters above the orebodies and is characterized by significant MgO mass gains, K₂O-Na₂O mass losses, and high alteration index values (e.g., chlorite-carbonate-pyrite index, alteration index). Similar alteration minerals (i.e., sericite-chlorite \pm talc assemblage) and chemical changes in both the footwall and hanging-wall rocks indicate that the two units were affected by the same hydrothermal system. The presence of talc in VMS deposits at Matagami is interpreted to be synvolcanic in origin (Costa



Subaqueous emplacement of the Watson rhyolite (WR). Onset of tuffaceous sedimentation on the seafloor related to an episode of district-scale andesitic ash deposition. The topography formed by the top of the rhyolite is draped by the Key Tuffite (KT). Synvolcanic faults locally form in extensional regime.

Onset of hydrothermal activity during ongoing tuffaceous sedimentation. Metal-bearing fluids ascend steep synvolcanic faults and are focused by the structural porosity of the conduits. Mixing with seawater occurs in a subseafloor environment, leading to sulfide replacement within the footwall rhyolite.



Emplacement of the Dumagami rhyodacite (DR) in an environment of tuff sedimentation while the hydrothermal system is still at its peak. Hydrothermal alteration continues in the hanging-wall in conjunction with the progressive decline of the system.

Emplacement of the upper portion of the Wabasse Group, including the Wabasse andesite (WA). Post-volcanic deformation episode related to regional N-S shortening generating structural modifications of the deposit, including a banded texture in the ore, the formation of oreshoots, folding of the units, fault reactivation and a possible internal remobilization of Cu.



Fig. 11. Schematic representation of successive stages in the evolution of the Perseverance deposit (north-south section of the Equinox orebody).

et al., 1983; Galley et al., 2007); the predeformation nature of talc at Perseverance is supported by the overprint of all alteration facies by the S_1 foliation. Mass-balance calculations also indicate that hydrothermal alteration in the hanging wall is less intense than that developed in the footwall. Radiometric dating of the footwall and hanging-wall units at respectively 2725.9 ± 0.8 and 2725.4 ± 0.7 Ma (Ross et al., 2014) supports the rapid emplacement of the Dumagami rhyodacite on top of the Watson rhyolite. The rhyodacite was most likely emplaced in an environment of tuff sedimentation and massive sulfide deposition (Fig. 11C). Hanging-wall alteration suggests that the hydrothermal system was still at its peak during emplacement of the rhyodacite and subsequently declined by the time the massive sulfides became buried. Other examples of massive sulfide deposits that recorded a declining hydrothermal activity during accumulation of the hanging-wall rocks include the Kuroko deposits (Iijima, 1974), Hellyer (Gemmell and Fulton, 2001), or Boundary (Piercey et al., 2014). According to this interpretation, it is unlikely that the hydrothermal system persisted long after emplacement of the rhyodacite to form stacked lenses higher in the volcanic succession.

Postdepositional deformation

The South Flank of the district has been previously described as a low strain area where deformation was accommodated by narrow brittle-ductile shear zones (Piché et al., 1993) and where VMS deposits have preserved their original characteristics (Lavallière et al., 1994). Other authors, including Roberts (1975), pointed out the structural complexity of the volcanic succession in proximity to the deposits of the South Flank area (i.e., Matagami Lake). At Perseverance, the presence of a penetrative schistosity and the development of folds in the host units indicate that the deposit was affected by postvolcanic deformation related to regional greenschist facies metamorphism. Primary relationships between mineralization and the host lithofacies were complicated by deformation, as illustrated by the flattening of massive sulfide orebodies parallel to the main schistosity S_1 .

Marked internal modifications of the massive sulfide lenses are illustrated in the deposit by the presence of folding and boudinage of the dikes, durchbewegung structures, and piercement veins. Dikes affected by folding in the sulfide assemblage have recorded significant strain and indicate a shortening on the order of 40%. The mineralogical banding developed at Perseverance is discordant to the subhorizontal volcanic succession and is closely associated with structurally emplaced elements (i.e., boudins and durchbewegung structures). These relationships suggest that the texture is also structural in origin and postdates the original ore characteristics. Spatial correlations between the mineralogical bands in the ore and the attitude of the schistosity in the host rocks indicate that these two fabrics formed under identical stress regimes, during the main event of deformation D_1 induced by regional north-south shortening. The transposition of sulfide ores subparallel to the main foliation is documented in other VMS deposits of the Abitibi subprovince (e.g., Doyon-Bousquet-LaRonde mining camp; Mercier-Langevin et al., 2004; Dubé et al., 2007).

Ore minerals in the lenses display contrasted behaviors related to their respective strengths—pyrite and magnetite

show evidence of brittle deformation, whereas chalcopyrite appears to have deformed in a ductile manner. Sphalerite displays a transitional behavior and was affected by annealing processes. Several workers documented the mechanical behavior of massive sulfide assemblages through experimental work for varying conditions of temperature, pressure, stress-differential and, strain-rate (Clark and Kelly, 1976; Cox, 1987; Marshall and Gilligan, 1987). Most of the sulfides except pyrite (i.e., galena, chalcopyrite, pyrrhotite, and sphalerite) are variably affected by cataclasis and dislocation flow processes at metamorphic temperatures and exhibit dynamic recrystallization under low-grade conditions (Marshall and Gilligan, 1993). Chalcopyrite and pyrrhotite behave in a ductile manner at least down to 200° and 240°C, respectively, depending on the confining pressure (Fig. 12; Clark and Kelly, 1976; Marshall and Gilligan, 1993). In contrast, pyrite and magnetite are more refractory to the stress and comparatively less ductile than the other sulfides over a wide range of pressure and temperature (Fig. 12). Pyrite deforms by brittle fracturing through pressure solution and cataclasis at low temperatures (McClay and Ellis, 1983; Craig et al., 1998); however, the mineral deforms by dislocation processes above 400°C (Cox et al., 1981). At Perseverance, for temperatures corresponding to greenschist facies in the range of 300° to 400°C, solid-state mechanical transfer related to ductile behavior was the dominant deformation mechanism in the sulfides (Fig. 12). Mechanical segregation in polymineralic

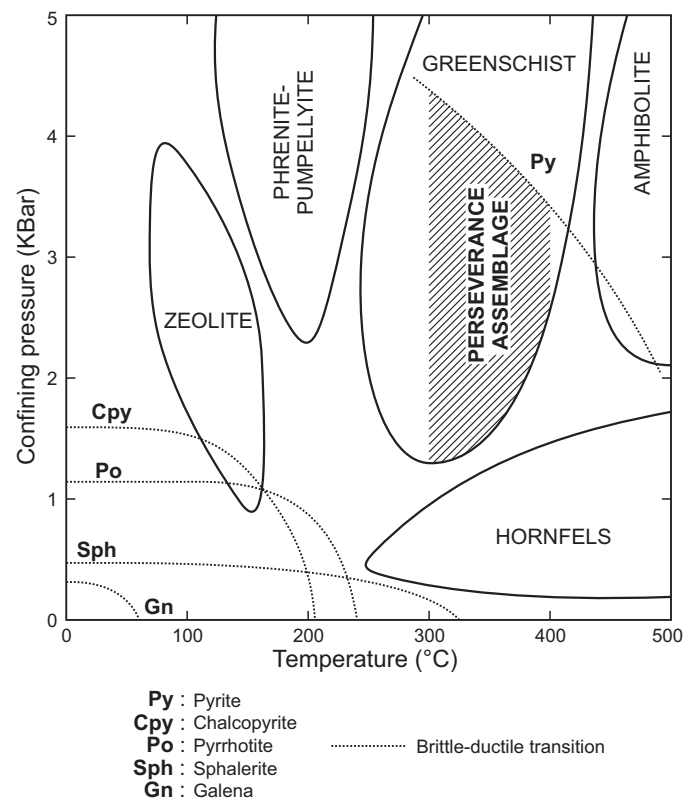


Fig. 12. Mechanical behavior of common base metal sulfides with their brittle-ductile transitions at 5% ductile strain before faulting, and indicative position of the Perseverance assemblage at greenschist facies conditions (modified from Marshall and Gilligan, 1987).

aggregates tends to produce monomineralic layers of minerals with different strength characteristics and deformation behavior. The development of a mineralogical banding in the orebodies likely resulted from the mechanical segregation of separate sulfides during ductile deformation (McDonald, 1970; Cowden and Archibald, 1987).

The strong structural modification recorded in the massive sulfides contrasts with a relatively weaker deformation in the host rocks of the deposit. Marshall and Gilligan (1987) have shown that common sulfides, except pyrite, have much lower effective viscosities than silicate rocks throughout the range of regional metamorphism. These minerals consequently behave in a more ductile fashion than more competent silicate rocks during deformation and favorably accommodate the strain as a result of rheology contrasts. Such contrast was most likely accentuated at Perseverance by the high proportion of sphalerite relative to pyrite in the orebodies, suggesting an influence of the primary ore composition on postdepositional deformation mechanisms. Local sharp top contacts between massive sulfides and the hanging-wall rhyodacite contrast with the usual stratigraphy of the deposit (i.e., presence of the Key Tuffite unit at this interface). The structural character of these contacts is underlined by piercement of the massive sulfides into the volcanic unit, folding, and the development of mineralogical bands. These relationships suggest that the upper boundaries of the massive sulfides at Perseverance have been locally affected by mechanical remobilization, in association with the formation of ore shoots (Fig. 11D). Although diverging from the parent mineralization, ore shoots at Perseverance do not significantly mask original geometric relationships and remain within the enveloping surface encompassing the parent body. Both the schistosity and folding recorded within altered rocks in the periphery of the orebodies suggest that hydrothermal alteration halos favorably accommodated the strain relative to least altered volcanic rocks during deformation.

Volcanogenic massive sulfide deposits commonly display mineral zonation induced by temperature variations and zone refining, resulting in chalcopyrite enrichment at the base and core of the lens (Lydon, 1984; Galley et al., 2007). While sphalerite displays a distinct zonation with Zn grades increasing upward and outward in the orebodies, the distribution of chalcopyrite is broadly scattered. Chalcopyrite constitutes one of the less competent minerals of the polymetallic assemblage during deformation and can be mechanically remobilized down to 200°C (Marshall and Gilligan, 1993). The systematic remobilization of the mineral relative to other sulfides and silicate elements indicates a spatial reorganization within the ore in response to ductility contrasts between materials. Evidence for the ductile behavior of chalcopyrite at Perseverance and the absence of a clear metal zonation in Cu within the orebodies suggests a possible internal redistribution of this metal during postdepositional deformation.

Conclusions

The Perseverance deposit is characterized by an atypical architecture relative to other deposits of the Matagami district due to the presence of four pipelike orebodies discordant to their near-horizontal host volcanic rocks. The reconstruction

of successive stages in the evolution of the deposit brings new insights into the mechanisms that controlled VMS deposition in the district. It also indicates that VMS deposits of the South Flank area have recorded a significant structural overprint during regional deformation.

Ore formation at Perseverance is interpreted to have occurred predominantly by subseafloor replacement of the footwall Watson rhyolite during the progressive deposition of the Key Tuffite on the seafloor. Subseafloor replacement was likely controlled by the structural porosity of steep synvolcanic structures, which promoted upward migration of hydrothermal fluids and the simultaneous infiltration of seawater. The hanging-wall Dumagami rhyodacite was emplaced while massive sulfide deposition and hydrothermal activity were still ongoing, leading to the development of pervasive hydrothermal alteration above the orebodies.

Primary relationships between the massive sulfides and the host lithofacies were overprinted by intense deformation during the main event of compression D_1 induced by regional north-south shortening. Deformation is controlled by competency contrasts related to different material rheologies within the sulfide assemblage and between the orebodies and their silicate host rocks. The tectonic overprint modified the shape of the lenses, generated secondary textures in the ore, including a deformation-induced mineralogical banding and produced structural ore shoots at the interface with host rocks. This episode of deformation also obliterated the distribution of less-competent minerals in the deposit and likely induced the remobilization of Cu.

The study provides useful guidelines for future VMS exploration strategies in the district. Pervasive hanging-wall alteration is associated with ore deposition and consequently, Mg enrichments combined with depletions of alkali elements should be carefully examined in the hanging walls of VMS targets. Additionally, alteration halos have accommodated most of the postore strain due to their lower competency and hydrothermal alteration is therefore spatially correlated with deformation despite the absence of a genetic relationship. The recognition of ductile deformation related to hydrothermal alteration in fertile volcanic rocks would aid exploration success.

Acknowledgments

This paper forms part of an M.Sc. thesis by the first author. Financial aid and logistical support for this project were provided by Glencore Canada Corporation (formerly Xstrata Zinc), Donner Metals, Mitacs Acceleration, and Consorem. We are grateful for numerous discussions with production and exploration staffs at Matagami, particularly R. Dussault, J. Drapeau, R. Nieminen, R. Brassard, and M. Dessureault, who helped in the work undertaken at the Perseverance mine and for access to unpublished data. The study has benefited from the contribution of M. Gauthier who is thanked for constructive discussions in the field. We also acknowledge reviews by J. Franklin and J. Hedenquist that helped to improve an early version of the manuscript. M. Laithier is thanked for her contribution in the preparation of the figures. *Economic Geology* reviewers Rodney Allen, Steve Piercey, and Dominique Genna are thanked for their reviews and suggestions, which have greatly improved the manuscript.

REFERENCES

- Adair, R., 2009, Technical report on the resource calculation for the Bracemac-McLeod discoveries, Matagami, Quebec: Vancouver, Canada, Donner Metals Ltd., National Instrument 43-101 Report, 194 p.
- Adam, E., Milkereit, B., and Mareschal, M., 1998, Seismic reflection and borehole geophysical investigations in the Matagami mining camp: Canadian Journal of Earth Sciences, v. 35, p. 686–695.
- Arnold, G., 2006, Geology and resource estimate of the Perseverance project, Matagami, Quebec: Toronto, Canada, Falconbridge Ltd., National Instrument 43-101 Report, 178 p.
- Barrett, T.J., and MacLean, W.H., 1994, Mass changes in hydrothermal alteration zones associated with VMS deposits of the Noranda area: Exploration and Mining Geology, v. 3, p. 131–160.
- Barrett, T., MacLean, W., Cattalani, S., and Hoy, L., 1993, Massive sulfide deposits of the Noranda area, Quebec. V. The Corbet mine: Canadian Journal of Earth Sciences, v. 30, p. 1934–1954.
- Beaudry, C., and Gaucher, E., 1986, Cartographie géologique dans la région de Matagami, Québec: Ministère de l'Énergie et des Ressources du Québec, Rapport MB 86-32, 147 p.
- Carr, P.M., Cathles, L.M., and Barrie, C.T., 2008, On the size and spacing of volcanogenic massive sulfide deposits within a district with application to the Matagami district, Quebec: Economic Geology, v. 103, p. 1395–1409.
- Clark, B., and Kelly, W., 1976, Experimental deformation of common sulphide minerals, in Strens, R.G.J., ed., The physics and chemistry of minerals and rocks: New York, Wiley, p. 51–70.
- Costa, U.R., Barnett, R.L., and Kerrich, R., 1983, The Matagami Lake mine Archean Zn-Cu sulfide deposit, Quebec: Hydrothermal coprecipitation of talc and sulfides in a sea-floor brine pool: Evidence from geochemistry, $^{18}\text{O}/^{16}\text{O}$, and mineral chemistry: Economic Geology, v. 78, p. 1144–1203.
- Cowden, A., and Archibald, N.J., 1987, Massive-sulfide fabrics at Kambalda and their relevance to the inferred stability of monosulfide solid-solution: Canadian Mineralogist, v. 25, p. 37–50.
- Cox, S., 1987, Flow mechanisms in sulphide minerals: Ore Geology Reviews, v. 2, p. 133–171.
- Cox, S.F., Etheridge, M.A., and Hobbs, B.E., 1981, The experimental ductile deformation of polycrystalline and single crystal pyrite: Economic Geology, v. 76, p. 2105–2117.
- Craig, J., Vokes, F., and Solberg, T., 1998, Pyrite: Physical and chemical textures: Mineralium Deposita, v. 34, p. 82–101.
- Davidson, A.J., 1977, Petrography and chemistry of the Key Tuffite at Bell Allard, Matagami, Quebec: M.Sc. thesis, Montreal, Canada, McGill University, 153 p.
- Debreil, J.A., 2014, Évolution volcanologique et chimico-stratigraphique du district minier de Matagami, Sous-Province de l'Abitibi, Québec: Ph.D. thesis, Québec, Canada, Institut National de la Recherche Scientifique, 301 p.
- Doyle, M.G., and Allen, R.L., 2003, Subsea-floor replacement in volcanic-hosted massive sulfide deposits: Ore Geology Reviews, v. 23, p. 183–222.
- Dubé, B., Mercier-Langevin, P., Hannington, M., Lafrance, G., Gosselin, G., and Gosselin, P., 2007, The LaRonde Penna world-class Au-rich volcanogenic massive sulfide deposit, Abitibi, Quebec: Mineralogy and geochemistry of alteration and implications for genesis and exploration: Economic Geology, v. 102, p. 633–666.
- Dubé, B., Mercier-Langevin, P., Kjarsgaard, I., Hannington, M., Bécu, V., Côté, J., Moorhead, J., Legault, M., and Bédard, N., 2014, The Bousquet 2-Dumagami world-class Archean Au-rich volcanogenic massive sulfide deposit, Abitibi, Quebec: Metamorphosed submarine advanced argillic alteration footprint and genesis: Economic Geology, v. 109, p. 121–166.
- Duuring, P., Bleeker, W., and Beresford, S., 2007, Structural modification of the komatiite-associated Harmony nickel sulfide deposit, Leinster, Western Australia: Economic Geology, v. 102, p. 277–297.
- Franklin, J., Gibson, H., Jonasson, I., and Galley, A., 2005, Volcanogenic massive sulfide deposits: Economic Geology 100th Anniversary Volume, p. 523–560.
- Galley, A.G., Hannington, M., and Jonasson, I., 2007, Volcanogenic massive sulphide deposits: Mineral deposits of Canada: A synthesis of major deposit-types, district metallogeny, the evolution of geological provinces, and exploration methods: Geological Association of Canada, Mineral Deposits Division Special Publication 5, p. 141–161.
- Gemmell, J.B., and Fulton, R., 2001, Volcanic, genesis, and exploration implications of the footwall and hanging-wall alteration associated with the Hellyer volcanic-hosted massive sulfide deposit, Tasmania, Australia: Economic Geology, v. 96, p. 1003–1035.
- Gemmell, J.B., and Herrmann, W., 2001, A special issue on alteration associated with volcanic-hosted massive sulfide deposits, and its exploration significance: Economic Geology, v. 96, p. 909–912.
- Genna, D., Gaboury, D., and Roy, G., 2014, The Key Tuffite, Matagami Camp, Abitibi greenstone belt, Canada: Petrogenesis and implications for VMS formation and exploration: Mineralium Deposita, v. 49, p. 489–512.
- Gibson, H.L., and Watkinson, D., 1990, Volcanogenic massive sulphide deposits of the Noranda cauldron and shield volcano, Quebec: Canadian Institute of Mining and Metallurgy Special Volume 43, p. 119–132.
- Gilligan, L., and Marshall, B., 1987, Textural evidence for remobilization in metamorphic environments: Ore Geology Reviews, v. 2, p. 205–229.
- Grant, J.A., 1986, The isocon diagram: A simple solution to Gresens' equation for metasomatic alteration: Economic Geology, v. 81, p. 1976–1982.
- Gresens, R.L., 1967, Composition-volume relationships of metasomatism: Chemical Geology, v. 2, p. 47–65.
- Hannington, M.D., Barrie, C.T., and Bleeker, W., 1999, The giant Kidd Creek volcanogenic massive sulfide deposit, western Abitibi subprovince, Canada: Preface and introduction: Economic Geology Monograph 10, p. 1–30.
- Iijima, A., 1974, Clay and zeolitic alteration zones surrounding Kuroko deposits in the Hokuroku district, northern Akita, as submarine hydrothermal-diagenetic alteration products: Mining Geology, v. 6, p. 267–289.
- Ioannou, S.E., and Spooner, E.T.C., 2007, Fracture analysis of a volcanogenic massive sulfide-related hydrothermal cracking zone, Upper Bell River Complex, Matagami, Quebec: Application of permeability tensor theory: Economic Geology, v. 102, p. 667–690.
- Ishikawa, Y., Sawaguchi, T., Iwaya, S., and Horiuchi, M., 1976, Delineation of prospecting targets for Kuroko deposits based on modes of volcanism of underlying dacite and alteration haloes: Mining Geology, v. 26, p. 105–117.
- Jolly, W.T., 1978, Metamorphic history of the Archean Abitibi belt: Geological Survey of Canada Paper 78-10, p. 63–78.
- Knuckey, M., Comba, C., and Riverin, G., 1982, Structure, metal zoning and alteration at the Millenbach deposit, Noranda, Quebec: Precambrian sulphide deposits, HS Robinson Memorial Volume: Geological Association of Canada Special Paper, v. 25, p. 255–295.
- Large, R.R., and Both, R.A., 1980, The volcanogenic sulfide ores at Mount Chalmers, eastern Queensland: Economic Geology, v. 75, p. 992–1009.
- Large, R.R., Gemmell, J.B., Paulick, H., and Huston, D.L., 2001, The alteration box plot: A simple approach to understanding the relationship between alteration mineralogy and litho-geochemistry associated with volcanic-hosted massive sulfide deposits: Economic Geology, v. 96, p. 957–971.
- Lavallière, G., Guha, J., and Daigneault, R., 1994, Cheminees de sulfures massifs atypiques du gisement d'Isle-Dieu, Matagami, Québec: Implications pour l'exploration: Exploration and Mining Geology, v. 3, p. 109–129.
- Liaghat, S., and MacLean, W.H., 1992, The Key Tuffite, Matagami mining district: Origin of the tuff components and mass changes: Exploration and Mining Geology, v. 1, p. 197–207.
- Lydon, J.W., 1984, Ore deposit models: Volcanogenic massive sulphide deposits. Pt. I: A descriptive model: Geoscience Canada, v. 11, p. 195–202.
- MacGeehan, P.J., and MacLean, W.H., 1980, Tholeiitic basalt-rhyolite magmatism and massive sulphide deposits at Matagami, Quebec: Nature, v. 283, p. 153–157.
- MacLean, W., 1984, Geology and ore deposits of the Matagami District: Canadian Institute of Mining and Metallurgy Special Volume 34, p. 483–495.
- 1990, Mass change calculations in altered rock series: Mineralium Deposita, v. 25, p. 44–49.
- MacLean, W., and Barrett, T., 1993, Litho-geochemical techniques using immobile elements: Journal of Geochemical Exploration, v. 48, p. 109–133.
- MacLean, W.H., and Kranidiotis, P., 1987, Immobile elements as monitors of mass transfer in hydrothermal alteration: Phelps Dodge massive sulfide deposit, Matagami, Quebec: Economic Geology, v. 82, p. 951–962.
- Maier, W., Barnes, S.-J., and Pellet, T., 1996, The economic significance of the Bell River Complex, Abitibi subprovince, Quebec: Canadian Journal of Earth Sciences, v. 33, p. 967–980.
- Marshall, B., and Gilligan, L.B., 1987, An introduction to remobilization: Information from ore-body geometry and experimental considerations: Ore Geology Reviews, v. 2, p. 87–131.
- 1989, Durchbewegung structure, piercement cusps, and piercement veins in massive sulfide deposits: Formation and interpretation: Economic Geology, v. 84, p. 2311–2319.
- 1993, Remobilization, syn-tectonic processes and massive sulphide deposits: Ore Geology Reviews, v. 8, p. 39–64.
- McClay, K., and Ellis, P., 1983, Deformation and recrystallization of pyrite: Mineralogical Magazine, v. 47, p. 527–538.

- McDonald, J.A., 1970, Some effects of deformation on sulfide-rich layers in lead-zinc ore bodies, Mount Isa, Queensland: *Economic Geology*, v. 65, p. 273–298.
- McPhie, J., Doyle, M., Allen, R., and Allen, R.L., 1993, Volcanic textures: A guide to the interpretation of textures in volcanic rocks: Hobart, Australia, Centre for Ore Deposit and Exploration Studies, University of Tasmania, 198 p.
- McQueen, K.G., 1987, Deformation and remobilization in some Western Australian nickel ores: *Ore Geology Reviews*, v. 2, p. 269–286.
- Mercier-Langevin, P., Dubé, B., Hannington, M.D., Davis, D.W., and Laffrance, B., 2004, Contexte géologique et structural des sulfures massifs volcanogènes aurifères du gisement LaRonde, Abitibi: *Ministère des ressources naturelles, de la Faune et des Parcs du Québec, ET 2003-03*, 47 p.
- Mercier-Langevin, P., Gibson, H.L., Hannington, M.D., Goutier, J., Monecke, T., Dubé, B., and Houlié, M.G., 2014, A special issue on Archean magmatism, volcanism, and ore deposits. Pt. 2. Volcanogenic massive sulfide deposits preface: *Economic Geology*, v. 109, p. 1–9.
- Mortensen, J.K., 1993, U-Pb geochronology of the eastern Abitibi subprovince. Pt. 1: Chibougamau-Matagami-Joutel region: *Canadian Journal of Earth Sciences*, v. 30, p. 11–28.
- Piché, M., Guha, J., and Daigneault, R., 1993, Stratigraphic and structural aspects of the volcanic rocks of the Matagami mining camp, Quebec: Implications for the Norita ore deposit: *Economic Geology*, v. 88, p. 1542–1558.
- Piercey, S.J., Squires, G.C., and Brace, T.D., 2014, Lithostratigraphic, hydrothermal, and tectonic setting of the Boundary volcanogenic massive sulfide deposit, Newfoundland Appalachians, Canada: Formation by sub-seafloor replacement in a Cambrian rifted arc: *Economic Geology*, v. 109, p. 661–687.
- Pilote, P., Debreil, J.-A., Williamson, K., Rabeau, O., and Lacoste, P., 2011, Révision géologique de la région de Matagami: Québec Exploration, Québec, Canada, 2011, Poster 276.
- Riverin, G., and Hodgson, C.J., 1980, Wall-rock alteration at the Millenbach Cu-Zn mine, Noranda, Quebec: *Economic Geology*, v. 75, p. 424–444.
- Roberts, R.G., 1975, The geological setting of the Matagami Lake mine, Quebec: A volcanogenic massive sulfide deposit: *Economic Geology*, v. 70, p. 115–129.
- Ross, P.-S., McNicoll, V.J., Debreil, J.-A., and Carr, P., 2014, Precise U-Pb geochronology of the Matagami mining camp, Abitibi greenstone belt, Quebec: Stratigraphic constraints and implications for volcanogenic massive sulfide exploration: *Economic Geology*, v. 109, p. 89–101.
- Sharpe, J.I., 1968, Geology and sulfide deposits of the Matagami area, Abitibi-East County: *Ressources Naturelles Québec Geological Report 137*, 122 p.
- Shriver, N., and MacLean, W., 1993, Mass, volume and chemical changes in the alteration zone at the Norbec mine, Noranda, Quebec: *Mineralium Deposita*, v. 28, p. 157–166.
- Vokes, F.M., 1976, A review of the base metal deposits of the Norwegian Caledonides: *Handbook of Strata-bound and Stratiform Ore Deposits*, v. 6, p. 79–128.
- Vokes, F.M., and Craig, J., 1993, Post-recrystallisation mobilisation phenomena in metamorphosed stratabound sulphide ores: *Mineralogical Magazine*, v. 57, p. 19–28.